Master's thesis

NTNU
Norwegian University of Science and Technology
Faculty of Engineering
Department of Marine Technology

Jørgen Gulpinar

Analysis of the Havfarm concept for extreme environmental loads

Master's thesis in Marine Technology
Supervisor: Jørgen Amdahl
Co-supervisor: Martin Slagstad
June 2021

NTNU
Norwegian University of
Science and Technology

Jørgen Gulpinar

Analysis of the Havfarm concept for extreme environmental loads

Master's thesis in Marine Technology
Supervisor: Jørgen Amdahl
Co-supervisor: Martin Slagstad
June 2021

Norwegian University of Science and Technology
Faculty of Engineering
Department of Marine Technology

NTNU
Norwegian University of
Science and Technology

Preface

This thesis is the concluding work of my studies of Marine Technology at the Norwegian University of Science and Technology. It is the culmination of the work carried out in the spring semester of 2021. It builds upon the project thesis written in the autumn of 2020. The thesis is intended for readers with some prior knowledge in the field marine technology.

I would like to first thank my supervisor Prof. Jørgen Amdahl for his guidance on this project. Without his help this thesis would not exist. I would also like to extend my gratitude to M.Sc. Vegard Holen whose prior work on the study of Havfarm 1 has been of great help, and whose work in modelling Havfarm 1 forms the basis for my work. Further, I would be amiss to not mention Ph.D candidate Martin Slagstad for his help with interpreting the results.

For posterity I would like to note that as I am writing this the world is currently recovering from the largest pandemic in recent history. While I as a Norwegian student has to a large extent been shielded against the effects of this pandemic, many have not. The official number is 173 million infected and 3.7 million known dead, and it is assumed that there are many more, as well as large economic, cultural and psychological ramifications. Please let this be a reminder that humankind is not invincible and that there are many problems yet to solve.

Trondheim, June 10, 2021

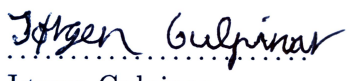

Jørgen Gulpinar

Abstract

Norwegian aquaculture has grown dramatically in the last decade, both in terms of fish volumes produced, but also the scale of the fish farms. One of these fish farms is Nordlaks's Havfarm 1. A large structure, almost 400m long, Havfarm 1 represents a change in Norwegian aquaculture towards larger structures and the use of more exposed locations.

In this thesis, an evaluation of this structure has been attempted by investigating the behaviour of a model established in a previous master project. In addition, a brief review of the structure concept has been presented, as well as a brief look at related literature. A recap of the modeling decisions made in the previous master project has also been given.

Methods of ULS analysis have been presented, with focus on the contour line method. The structure was analyzed using both frequency domain methods and time domain simulations. In order to perform this, the structural analysis program USFOS, has been used in conjunction with scripting in python.

Due to a lack of data on the metocean conditions of the location, the full contour line method was not employed. A scatter matrix with the necessary information was later obtained, but due to time constraints was not utilized. Instead the worst sea state was assumed based on limited information about the location, as well as test results from regular wave analysis. The short term distribution of the extreme heave response was then established using both frequency domain analysis and time domain analysis. The results from both analyses were then compared.

Sammendrag(Norwegian)

Norsk havbruk har hatt en dramatisk vekst i det siste tiåret, både i form av økte produksjonsvolum, men også i størrelsen på oppdrettsanleggene. En av disse oppdrettsanleggene er Nordlaks sin Havfarm 1. Det er en stor struktur, nesten 400 m lang, og representerer en endring i Norsk havbruk, med bruk av større strukturer og mer eksponerte områder.

I denne oppgaven har det blitt forsøkt å evaluere strukturen, ved å ta i bruk en modell etablert i en tidligere masteroppgave. I tillegg har det blitt presentert en kort evaluering av det strukturelle konseptet, samt en kort gjennomgang av relatert litteratur. En oppsummering av valgene gjort i modelleringsprosessen i den tidligere oppgaven er også med.

Metoder brukt i ULS analyse har blitt presentert, med fokus på konturlinjemetoden. Strukturen ble analysert med bruk av både frekvensplan metoder og tidsdomene simuleringer. For å gjennomføre dette har det strukturelle analyse programmet USFOS blitt brukt, sammen med skripting i python.

På grunn av begrenset informasjon om værtilstanden i området, ble ikke den fullstendige konturlinjemetoden brukt. En spredningsmatrise med den nødvendige informasjonen ble anskaffet ved et senere tidspunkt, men har ikke blitt brukt på grunn av tidsbegrensninger. Isteden ble det gjort antagelser om den verste sjøtilstanden basert på begrenset informasjonen om området samt resultater fra regulær bølge analyse. Den kortsiktige fordelingen av ekstremresponsen ble så etablert, ved bruk av både frekvensdomene analyse og tidsdomene analyse. Resultatet fra begge analysene ble så sammenlignet.

Contents

Preface i

Abstract i

Sammendrag(Norwegian) iv

List of Figures ix

List of Tables xi

1 Introduction 1
- 1.1 Thesis outline . . . 1
- 1.2 Problem definition . . . 6

2 Presentation of the Havfarm concept 7

3 Litterature review 9
- 3.1 Relevant papers . . . 9
- 3.2 Rules and regulations . . . 9
- 3.3 Wave attenuation . . . 10

4 Theoretical background 11
- 4.1 Limit state design . . . 11
- 4.2 Methods for predicting characteristic loads . . . 13
  - 4.2.1 Regular wave analysis . . . 13
  - 4.2.2 Design wave method . . . 13
  - 4.2.3 Stochastic analysis . . . 13
- 4.3 Wave spectra . . . 17
  - 4.3.1 Irregular waves . . . 17
  - 4.3.2 The JONSWAP spectrum . . . 18
- 4.4 Damped eigenfrequency . . . 19

5 Vegard Holen's Havfarm 1 model 21
- 5.1 USFOS . . . 21
- 5.2 Holen's Model . . . 21
  - 5.2.1 Changes to the final concept . . . 21
  - 5.2.2 Mass distribution . . . 24
  - 5.2.3 Loading . . . 25
  - 5.2.4 Damping . . . 25
  - 5.2.5 Mooring . . . 27
  - 5.2.6 Net pens . . . 28
  - 5.2.7 Comments on the model . . . 29

6 Analyses of the model **31**
6.1 Preliminary studies 31
6.1.1 Decay test 31
6.2 Investigating model behaviour 36
6.2.1 Establishing a transfer function 36
6.2.2 Net-pen model 39
6.2.3 Changes in the wave height 40
6.2.4 Measuring points 42
6.2.5 The significance of current 43
6.2.6 Regular waves with 6 meter wave height 47
6.3 Stochastic analysis in frequency plane 49
6.4 Stochastic analysis in time domain 51
6.4.1 Comparison between frequency and time domain 52

7 End remarks **55**
7.1 Conclusions 55
7.2 Recommendations for further work 56

Bibliography **57**

List of Figures

2.1 3D model of Havfarm 1 . . . 7

4.1 Example of q-probability contours[10] . . . 17

5.1 Holens model shown in USFOS GUI . . . 22
5.2 Final concept[17] . . . 22
5.3 Nodal masses and fill ratio of bottom pontoon[11] . . . 24
5.4 The relative importance of wave forces as a function of wave and structure dimensions.[8] . . . 26
5.5 Example of a hysterisis curve[12]. . . . 27
5.6 The modelled net pens . . . 28

6.1 Location of the measuring node . . . 32
6.2 Vertical displacement as a function of frequency . . . 33
6.3 Vertical displacement history . . . 33
6.4 Rotation displacement as a function of frequency . . . 34
6.5 Rotation over time . . . 34
6.6 Wave corresponding to a period of 23.4 seconds . . . 36
6.7 Initial transfer function . . . 37
6.8 Second transfer function . . . 37
6.9 History plot of heave motion of the measuring node. H = 0.1m and T = 5.82s . . 38
6.10 Third attempt at transfer function . . . 38
6.11 RAO, H = 0.1m, Current = 0.75 m/s Net pens . . . 39
6.12 RAO, H = 0.1m, Comparison of the models, Current = 0.75m/s . . . 40
6.13 Rough classification of when different load components are of importance. . . . 41
6.14 RAO, Waveheight of 1m, Current = 0.75 m/s, Comparison of net vs. no net . . . 41
6.15 RAO, Current = 0.75 m/s, Comparison of wave heights . . . 42
6.16 Position of the measuring points. . . . 42
6.17 Difference between measuring points, without net pens, H = 1 m . . . 43
6.18 Difference between measuring points, with net pens, H = 1 m, without current . 43
6.19 H=0.1m, No net, Current vs. No current . . . 44
6.20 H=0.1m, T = 5.82 s, No net, Time history of the heave motion . . . 44
6.21 H=0.1m, No net, Comparison of cutoff and current . . . 45
6.22 H=0.1m, Net, Comparison of cutoff and current . . . 45
6.23 H=0.1m, No net, Comparison of cutoff for both net and no net . . . 46
6.24 H=1m, Both models, Comparison of current vs. no current . . . 46
6.25 Both models, Comparison of wave heights without current . . . 47
6.26 RAO, H=6m, No net model . . . 48
6.27 H=1m, Both models, Comparison of current vs. no current . . . 48
6.28 JONSWAP spectrum, $H_s = 6$m, $T_p = 14.5$s . . . 49
6.29 Response spectrum, $H_s = 6$m, $T_p = 14.5$s . . . 50
6.30 Response height distribution, $H_s = 6$m, $T_p = 14.5$s . . . 50

6.31 Distribution of the largest response amplitude, H_s = 6m, T_p = 14.5s, 3 hour duration 52
6.32 Comparison of extreme value distributions, H_s = 6m, T_p = 14.5s, 3 hour duration 52

List of Tables

2.1 Key dimensions 7

4.1 Environmental load combinations as proposed by DNV GL[4] 12

5.1 Model dimensions 22
5.2 Cross section dimensions [m] 23
5.3 Material properties 23
5.4 Mass distribution 24
5.5 Drag and mass coefficients 25
5.6 Structural damping parameters 27
5.7 Net pen dimensions 28

6.1 The pitch results of the decay test. 35
6.2 Wavelengths corresponding to the natural frequencies. 35
6.3 Results: Regular airy wave, period = 40 s 39

Chapter 1

Introduction

As of 2021 humanity encompasses 7.7 billion souls, and UN projections estimate that we will pass 8 billion people in 2023, just two years time from now. Further it is expected that the world population in 250 will encompass 9.7 billion people and is expected to peak around the end of the century.[18] With so many mouths to feed an expansion in the food production is necessary.

While the worlds oceans have been a great source of food in the past, in recent decades there has been signs that the global fish population has been declining[23]. One solution to this problem could be an expansion into aquaculture. This is the route Norwegian authorities has decided to follow. In Norway there has long been a tradition for aquaculture, but mostly small scale, sometimes family operations. Only in recent decades has there been a large up-scaling of the production.

Due to large economic growth and expansion, suitable locations for conventional aquaculture became less available. This in connection with problems of fish escape and sea lice, prompted the industry and government to look for solutions. As a consequence the government decided that new licenses would only be given to companies trying out new concepts, as a measure to stimulate technological development. This has resulted in many interesting solutions, both on land and at sea. Havfarm 1 is one of these, taking on the challenge of more exposed waters. Such a structure must withstand more severe loads than what a conventional fish farm in calm waters would have to. Havfarm 1 or "Jostein Albert" as it has been named was completed, towed and made operational throughout summer and fall of 2020.

This master thesis will examine the concept from a structural design point of view, in an effort to contribute to the shared knowledge of large aquaculture structures. From a marine structures perspective the structure represents a sort of re-imagination of already well developed technology from offshore oil, but also something new and different.

1.1 Thesis outline

Here the original project description is presented along with the original scope. Note that the scope has changed somewhat, mostly due to the lack of contact with 7waves.

NTNU
Norges teknisk-naturvitenskapelige universitet
Institutt for marin teknikk

Master thesis 2021

for

Stud. Techn. Jørgen Gulpinar

Analysis of the Havfarm concept for extreme environmental loads

Analyse av Havfarm konseptet utsatt for ekstreme miljølaster

Marine fish farming is in rapid development. Dimensions are increasing and locations are being moved to areas exposed to more energetic waves and stronger currents. This leads to several challenges: Strong currents can cause large net deformations and affect largely the hydroelastic behaviour of the cage. Wave overtopping may occur in during extreme waves, so nonlinear effects matter. Viscous effects are essential for the loading on the net structures, as well as the wake inside the cage. Another issue is the effect of biofouling on the net loading. Waves and currents are of concern for the volume within the fish cage and the design of mooring lines.

Failure of fish farms, with large-scale fish escape to the level experienced in the past, will not be tolerated by the society. New and extreme loading scenarios need to be properly designed for by means of "*first principles"* methods to meet required safety levels and performance.

Rational design methods have been applied the design of Salmar's Ocean Farm 1 and Nordlaks' Havfarm1. The design is to a large degree based on principles and experience gained in the offshore oil and gas industry as regards fatigue and ultimate strength assessment. Although the structural performance is governed by effects that are similar to those for floating offshore structures, notable differences exist, e.g. the large size compared to predominant wave lengths, very location dependent wave and current conditions, current is

generally more important, sloshing loads in closed or semi-closed compartments, and loads from the fish net.

The Havfarm1 fish farm concept has recently been installed outside the island Hadsel in Vesterålen, with a design sea state of H_s = 6 m. Plans are now being made to move fish farming into even more hostile waters. An important issue is to balance the demand for relatively calm wave conditions inside the farm to create a sustainable environment for the fish stock with requirements to strengthening of the structural members of the fish farm

The intention of this work is to investigate possible structural solutions to create reduced wave kinematics inside Havfarm concept for exposed waters and their impactson loads and load effects.

The work is proposed carried out in the following steps:

1) Describe the Havfarm1 concept and discuss the particular challenges with regards to loads and load effects that this concept may face. Conduct a thorough evaluation of the model that is used in the simulations with USFOS. It is envisaged that the fish net does not need to be included in the model. Clarify relevant environmental conditions that may be critical for the structure. The maximum deviation between fish farm heading and direction of incoming waves shall be established.

2) Discuss various grid solutions for wave attenuation in the upper half of the sides in the fish farm structures. What methods are available to estimate the wave kinematics inside the structures and the forces transferred to the grid. In agreement with supervisors select analysis methods for further use in response calculations.

3) Perform eigenvalue analysis of the fish fram, and on this basis discuss the expected significance of structural dynamics.

4) Conduct analysis of the fish farm in regular waves and in irregular seas. Estimate the maximum values of selected response parameters, e.g. by means of the contour line method.

5) Evaluate potential consequences of rupture in the grid structure. Can the fish net be damage by a failed member?

6) If time permits, evaluate the consequences of impact from ships or a drifting objects. Estimate the residual strength of the damaged structure with voids flooded.

7) Conclusions and recommendations for further work in the master thesis project.

Literature studies of specific topics relevant to the thesis work may be included.

The work scope may prove to be larger than initially anticipated. Subject to approval from the supervisors, topics may be deleted from the list above or reduced in extent.

In the thesis the candidate shall present his personal contribution to the resolution of problems within the scope of the thesis work.

Theories and conclusions should be based on mathematical derivations and/or logic reasoning identifying the various steps in the deduction.

The candidate should utilise the existing possibilities for obtaining relevant literature.

Thesis format
The thesis should be organised in a rational manner to give a clear exposition of results, assessments, and conclusions. The text should be brief and to the point, with a clear language. Telegraphic language should be avoided.

The thesis shall contain the following elements: A text defining the scope, preface, list of contents, summary, main body of thesis, conclusions with recommendations for further work, list of symbols and acronyms, references and (optional) appendices. All figures, tables and equations shall be numerated.

The supervisors may require that the candidate, in an early stage of the work, presents a written plan for the completion of the work. The plan should include a budget for the use of computer and laboratory resources which will be charged to the department. Overruns shall be reported to the supervisors.

The original contribution of the candidate and material taken from other sources shall be clearly defined. Work from other sources shall be properly referenced using an acknowledged referencing system.

The report shall be submitted in two copies:
- Signed by the candidate
- The text defining the scope included
- In bound volume(s)
- Drawings and/or computer prints which cannot be bound should be organised in a separate folder.
- The report shall also be submitted in pdf format along with essential input files for computer analysis, spreadsheets, MATLAB files etc in digital format.

Ownership
NTNU has according to the present rules the ownership of the thesis. Any use of the thesis has to be approved by NTNU (or external partner when this applies). The department has the right to use the thesis as if the work was carried out by a NTNU employee, if nothing else has been agreed in advance.

Thesis supervisor
Prof. Jørgen Amdahl
PhD Martin Slagstad

Contact person at 7Waves:
Ole Harald Moe

Deadline: June 10, 2021
Trondheim, Januar 20, 2021

Jørgen Amdahl

1.2 Problem definition

This project was originally envisioned to be undertaken in cooperation with the company 7waves, which have been tasked with structural analysis of the structure. However, this agreement fell through. Therefore it was necessary to somewhat redefine the scope.

The central objective of this project has been to evaluate the dynamic behaviour of the structure, as well as estimate the maximum response. Previous master student Vegard Holen created a computer model of the structure, based on early design documents made available to him by Nordlaks/NSK ship design. His thesis was delivered in 2017. This model has been the basis for analysis in this master thesis.

It was of interest to evaluate the behaviour of this model, in order to say something about the Havfarm 1 concept. As such it was a point to investigate the dynamic behaviour of the model, both with and without the net pens. The analysis was to be conducted in both regular and irregular sea, and an estimate of the maximum response were to be established. Little to no communication has been had with 7waves during the project, except for some meetings between a contact person and the supervisor.

It was also envisioned that the work would answer if the structure could handle larger environmental loads, i.e. more exposed waters. If the structure were to be moved to more exposed waters, it would be necessary to reduce the waves internally, in order for the fish to be comfortable. Therefore a literature review of wave attenuation methods were undertaken.

This master thesis contains the following:

- Short description of Havfarm 1
- Literature study into:
  - Previous master theses and papers, published by the Department of Marine technology, NTNU
  - Current rules and regulations for design of fish farms and relevant offshore rules
  - Methods of wave attenuation
- Presentation of the methodology of limit state design, with focus on ULS utilization. Some related theory is also presented.
- Recap of the modeling decisions made by Vegard Holen and an evaluation of his work in modeling the structure.
- Decay tests in order to obtain the natural periods has been undertaken.
- Evaluation of the model behaviour when subjected to regular waves.
- Estimation of the maximum heave response using frequency domain analysis, and time domain analysis.
- Recommendations for further work.

Chapter 2

Presentation of the Havfarm concept

The owners of Havfarm 1, now Havfarmen "Jostein Albert", is Nordlaks. They are a large actor in norwegian aquaculture and in 2019 they had a total revenue of a little more than 3 billion NOK. The structure was designed by the company NSK ship design, a norwegian company specializing in the design of ships. Nordlaks give the following information about the fish farm[16] :

Dimension	Value
Length	385 m
Width	59.5 m
Height	37.75 m
Capacity	10 000 tonnes of fish

Table 2.1: Key dimensions

The structure can be categorized as something between a ship and a semi-submersible. It has been optimized for internal space, and inside the "hull" 6 net pens are suspended which will house the fish. The crew will be housed in the back. The farm is equipped with rail going carts designed to help the crew work more effectively without the need for help from ships. It is all powered by electricity from land cables.[16]

The fish farm is placed 5 km southwest of Hadseløya in Hadsel municipality in vesterålen. It is turret moored in the front, similar to a *Floating production storage and offloading unit*(FPSO). It has 11 anchors each weighing 22 tonnes, with a maximum capacity between 300-450 tonnes. The anchor are placed in 3 groups, with 4 anchors in the southwestern and northwestern group and 3 in the eastern group.

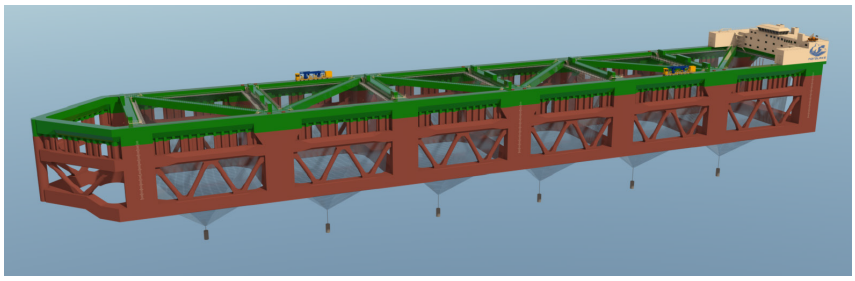

Figure 2.1: 3D model of Havfarm 1

The placement of the farm, while still close to shore, is in a significantly more exposed location than conventional farms. Both large waves and strong winds from the west, originating in the norwegian sea will affect it. Considering the large draft of the structure, it can be said that wind loads will only be of minor importance. More important are current and wave loads.

As it is turret moored, it will swivel around the central turret resulting in mostly head sea. Because of this, the largest motions the structure will experience is in surge, heave and pitch. When the structure is in service, a crew will be working aboard the vessel. Large motions and accelerations should therefore be avoided. In addition it is necessary to avoid large motions in order to ensure a good environment for the fish.

Chapter 3

Litterature review

As mentioned in the introduction, there has been a push for innovation in Norwegian aquaculture. This includes a considerable amount of research into the topic by both private companies and research institutions. Additionally, previous knowledge acquired in offshore oil and gas has been applied to this field. This chapter is a review off some relevant scientific literature as well as some relevant rules and regulations. The review of literature on wave attenuation is presented last. Note that, what is presented here is not a comprehensive review of relevant literature.

3.1 Relevant papers

In 2017 master of science Vegard Holen, delivered his master thesis on ultimate limit state analysis of the the Havfarm concept. The intention of the thesis was to investigate if the, then proposed, Havfarm concept would be able to pass ULS criteria. However, at the time of delivery the Havfarm 1 concept was still at an early stage of design. At the time of writing, the fish farm has been built, towed to Norway and is in the beginning of it's production. Holen placed much focus on developing a finite element model of the Havfarm concept, and much time was devoted to modeling the net pens. His master thesis[11] has been a source of guidance in this project and a valuable basis to build upon. The model he developed has been used as a basis for investigations into the USFOS program and behaviour of Havfarm 1.

Pål Takle Bore and Jørgen Amdahl[2] wrote a paper proposing methods for determining conditions relevant for the ultimate limit state at an exposed aquaculture location. The paper gives a detailed description of how one would do this using the location of SalMar/Ocean Farming's "Ocean Farm 1". In the paper the contour line method, directional model and JONSWAP spectrum were applied.

Martin Slagstad et al.[3] undertook an investigation into the validity of using simplified methods for assessing fatigue damage, when applied to exposed fish farms. They found that using a long term Weibull distribution to estimate the fatigue damage greatly underestimates the damage. It can therefore not be recommended. However further study might yield a refined method able to accurately predict the damage.

3.2 Rules and regulations

The NYTEK regulation governs the technical standards of floating aquaculture facilities. The purpose of the regulation is to contribute to preventing fish escape by securing sound technical standards of the facilities[9]. The regulation states that all aquaculture facilities shall be held to the criteria set forth in the Norwegian standard NS 9415[20]. In short it can be stated that the

design criteria given in this standard are good guidelines for conventional fish farms. However, they are not strict nor comprehensive enough for concepts like Havfarm 1, which are larger and faces harsher conditions.

DNV is a norwegian based classification society. Starting in 2017, they publish their own rules for classification of offshore fish farms, DNVGL-RU-OU-0503[6]. The newest revision at the time of writing was published in July of 2020, and contain requirements to different types of offshore fish farms. The rules differentiates between different concepts. In terms of structural design they list the following types:

- Ship-shaped type
- Column-stabilized type
- Self-elevating type
- Cylindrical type
- Deep draught type
- Concrete structures

In this case we are dealing with a collumn stabilized design. The classification rules refer to much of DNV GL's alrady existing rules and recommended practises related to offshore installations.

3.3 Wave attenuation

If the structure is to operate in deeper and more open waters, an important issue is that of internal waves in the net pens, in addition to currrents. An investigation into methods of both current and wave attenuation was therefore undertaken. The search was conducted using both google scholar and Oria. Terms used were: Surface wave attenuation, water wave attenuation, wave attenuation grid structure. The search yielded a few articles on the subject of wave attenuation by the use of porous barriers. The most relevant and cited paper found was: *Scattering and radiation of water waves by permeable barriers* by M. M. Lee and A. T. Chwang published in 2000 in the Scientific journal *Physics of fluids*.

The paper considers the two-dimensional problems of scattering and radiation of small-amplitude water waves by thin vertical porous plates in finite water depth. In addition, the performance of such barriers as breakwaters were also measured. In it, the researchers found that a porous barrier can reduce the impinging hydrodynamic wave forces acting on it, and at the same time maintain a reasonably good performance when it is used as a breakwater or wavemaker.[14]

Lee And Chwang references the work of F.Ursell, W. R. Dean, W. E. Williams and others, as sources on how barriers can be used for the purposes of wave attenuation, as well as methods to calculate the effect. Further investigation into methods of wave attenuation for the purposes of use with large offshore fish farms, should begin here.

Chapter 4

Theoretical background

In this chapter some theory is presented, in order for the reader to understand the methods used in the chapter on the dynamic analyses. The chapter presents limit state design and methods for establishing ULS utilization, methods of predicting characteristic loads, transfer functions and wave spectra, with weight on the JONSWAP spectrum.

4.1 Limit state design

Any structure, be it a bridge, oil platform or plane will be subjected to a variety of loads and deformations. These loads vary in both magnitude and frequency. In the design process, it is necessary that we account for these loads, and make sure the structure is able to resist them throughout its lifetime.

In structural design there are several design philosophies underlying various codes and standards. In the offshore industry there has been a shift from *Allowable strength design* (ASD/WSD,) to *limit state design* also known as the *load and resistance factors design* (LRFD). Torgeir Moan states in his compendium[15], when discussing limit state design, that: "The basic principle of the design verification is to ascertain that the structure or its elements do not reach any particular state (failure mode), called a limit state, in which it infringes one of the criteria governing its performance or use." The limit states used in current codes are split into four categories:

- Serviceability Limit States - SLS
- Ultimate Limit States - ULS
- Progressive Collapse Limit States - PLS
  - Also known as Accidental Limit States - ALS
- Fatigue Limit States - FLS

In this thesis only ULS will be discussed. To ensure that the limit state is not reached, it is necessary to determine the loads acting on the structure, determine the effects of said loads, determine the structure's resistance to these effects, and select materials and connections such that the resistance exceeds the load effects. In short:

$$S_d \leq R_d \tag{4.1}$$

where S_d is the design load effects and R_d is the design resistance. It is important to recognize that these quantities will be uncertain. Determination of the loads (Q) will have uncertainty due to measurement, the same is true for material resistance(f), as well as uncertainty stemming

from calculations etc. To account for this uncertainty, safety factors are introduced for both material resistance γ_m, and load effects γ_f. Equation 4.1 can then be written as:

$$S(\gamma_f Q_c) \leq R(\frac{f_c}{\gamma_m}) \tag{4.2}$$

The design process will in most cases be an iterative process. A concept is first proposed, and the loads acting on it must be found, it resistance to this load determined, and if insufficient (or to sufficient) the design must be changed and so on. The challenge is determining what loads and load combinations the structure will be affected by, and how these affect the structure. The structural codes give requirements for which load combinations must be looked at. In the case of Havfarm 1, the dynamic loads which are expected to most affect the structure, in both ULS and FLS consideration, are wave loads.

According to regulations, the environmental actions that we are to design against must be determined according to certain probabilities of exceedance. The probabilities of exceedance differs according to the limit state criteria. In ULS criteria the load combination must have a probability of exceedance equal to or less than 10^{-2}. It is most unlikely that there exists a joint probability distribution for all load combinations. As stated earlier, the codes therefore contain sets of environmental actions that should be considered simultaneously. The combinations of environmental actions proposed by DNV GL is given in table 4.1

Limit state	Wind	Waves	Current	Ice	Sea level
ULS	10^{-2}	10^{-2}	10^{-1}		10^{-2}
	10^{-1}	10^{-1}	10^{-2}		10^{-2}
	10^{-1}	10^{-1}	10^{-1}	10^{-2}	Mean water level
ALS	Return period not less than 1 year	Return period not less than 1 year	Return period not less than 1 year	Return period not less than 1 year	Return period not less than 1 year

Table 4.1: Environmental load combinations as proposed by DNV GL[4]

The ocean surface is in general not very easy to describe by using a deterministic model. If one were to observe the surface elevation at one spot for a given time interval, and then repeat the observation, it would be seen that the two time histories would be quite different. However, the mean wave height and mean wave period would be very similar. Because of this it is more useful to describe the surface process as a stochastic process. In the north sea it is common practise to split the time history in three hour long sea states, which within the process is assumed stationary as well as ergodic. The sea state can then be characterized by the significant wave height H_S, and spectral peak period T_p.

4.2 Methods for predicting characteristic loads

There are several methods for predicting the structural loads and load effects. The choice of method depends to a large extent on the nature of the response problem under question [10]. In general there can be said to be 3 methods for determining the governing load effects due to waves:

- Regular wave analysis
- Design wave analysis
- Stochastic analysis

4.2.1 Regular wave analysis

The regular wave analysis is presented in NS9415 and is the governing method for analysing conventional fish farm. The method can be said to be quite simple and not really adequate for non-conventional fish farms. In short the sea is modeled as a regular Airy wave, with the wave height equal to:

$$H = H_{max} = 1.9 \cdot H_s \tag{4.3}$$

The period is taken to be the peak period T_p. The significant wave height must have a return period of 50 years according to NS9415. In the offshore industry, standards require a 100-year return period. The response of the structure to this wave is then calculated.

4.2.2 Design wave method

For a quasi-static structure where the response is more or less defined by the instantaneous external loads, the design wave method is useful. The input to the analysis is either, the q-probability wave height and an associated unfavourable wave period, or a q-probability crest height and the associated mean wave period. By q-probability wave height it is meant the wave height with a probability of exceedance less or equal to q, e.g 10^{-2}. The most common approach has been to describe the waves using a stokes 5^{th} order profile. The extreme wave profile is reasonably well described using stokes 5^{th} order profile, as long as the wave is not close to breaking. Stokes waves can be seen as an extension of Airy waves, accounting for higher order effects. The wave is then stepped trough the structure, calculating the loads and response for each time step. The q-probability response is then taken to be the maximum value obtained during the process.[10]

This method should in principle only be applied when the instantaneous response is independent of the previous load history, i.e. when the effects of dynamics can be neglected. This means the method should only be used to analyse fixed structures. However, one can account for a small effect of dynamics, by considering the structure as a simple, single degree of freedom system and determining the *Dynamic amplification factor, DAF*. One then multiplies the q-probability response with this factor. The damping should be taken as around 1-2% of critical, since it will be only structural damping present. If the DAF is larger than 1.1 a more accurate method should be used to determine the dynamic amplification.

Since the Havfarm concept is definitively not a fixed structure, this method is not applicable in determining the characteristic loads and load effects.

4.2.3 Stochastic analysis

Stochastic analysis is employed when the behaviour of the structure depends both on the wave height and the wave period. If the structural response also depends on the previous wave history,

stochastic long term analysis is the most consistent method for predicting the characteristic response.

There are several methods of undertaking stochastic analysis. One method relies on determining the long term distribution of the response, and is dubbed stochastic long term analysis. Further differences in this method comes down to how one describes this long term distribution. Haver[10] presents 4 options:

One may consider the long term distribution of:

1. The individual maxima or cycle width of the target response process. This method is convenient for fatigue assessment based on S-N curves
2. The three hour maximum. As previously stated this is commonly used in the north sea at the Norwegian continental shelf.
3. The storm maximum response. Instead of considering all sea states, only consider those above a certain threshold. This method should be applied in hurricane dominated areas.
4. The annual extreme value of the target response. This method is less reasonable due to the assumption that the annual maximum response will be present in the annual maximum storm. It also requires at leas 50 years of metocean data.

Consider method two. The long term distribution of the three hour maximum X_{3h}, is given by:

$$F_{X_{3h}}(x) = \int_h \int_t F_{X_{3h}\backslash H_s T_p}(x\backslash h,t) f_{H_s T_p}(h,t) dt dh \tag{4.4}$$

$f_{H_s T_p}(h,t)$ is the long term distribution of the sea state parameters H_s and T_p, while $F_{X_{3h}\backslash H_s T_p}(x\backslash h,t)$ is the short term cumulative distribution of the three our maximum, given by the sea state parameters.

The long term distribution of the sea state parameters must be obtained from reliable observational data for the given location. The short term distribution is usually more challenging. If the problem can be said to be linear, it is quite simple to obtain the distribution. This method of obtaining the short term response is known as frequency domain analysis. If there is non-linearity involved it could be significantly more challenging. It will then be necessary to solve in time domain.

Frequency domain

If the mechanical system can be said to be linear, the relation between the response and load, in the frequency domain, is given by:

$$x_0(\omega) = H_M(\omega) F_0(\omega) \tag{4.5}$$

$x_0(\omega)$ is the response amplitude, $F_0(\omega)$ the load amplitude and $H_M(\omega)$ is called the mechanical transfer function. All are dependent on the wave frequency ω.

Further, if the relationship between load and wave amplitude is linear, it is given as:

$$F_0(\omega) = H_H(\omega) \cdot \zeta_0(\omega) \tag{4.6}$$

$\zeta_0(\omega)$ is the wave amplitude and $H_H(\omega)$ the hydrodynamic transfer function.

This can be rewritten to:

$$x_0(\omega) = H_M(\omega) \cdot H_H(\omega) \cdot \zeta_0(\omega) = H_x(\omega) \cdot \zeta_0(\omega) \tag{4.7}$$

Examining the surface elevation, it is possible to show that the process can be described using an energy spectrum, $S_\zeta(\omega)$, assuming we can model the surface elevation as a Gaussian process. Assuming the response is linearly dependent on the wave elevation, the response can be expressed as an energy spectrum dependent on the wave frequency, ω. The relation between the wave spectrum, $S_\zeta(\omega)$, and response spectrum, $S_x(\omega)$, is given as a function of the transfer function, $H_x(\omega)$:

$$S_x(\omega) = H_x(\omega)^2 \cdot S_\zeta(\omega) \tag{4.8}$$

Note that the transfer function in equation 4.8 expresses the relationship between the response and wave elevation, while the transfer function in equation 4.5 expresses the relationship between the response and load.

Since the response is linearly dependent on the surface elevation and the surface elevation is a Gaussian process, the response is also a Gaussian process. It can be shown that the response amplitude therefore is Rayleigh distributed, and further that the maximum response amplitude found in the sea state is Gumbel distributed. It is this maximum response we are ultimately interested in. Using a Gumbel model the distribution of the maximum response in a 3 hour sea state is given as[10]:

$$F_{X_{3h}|H_sT_p}(x|h,t) = \{1 - exp\{-\frac{1}{2}(\frac{x}{\sigma_x(h,t)})^2\}\}^{\eta_{3h}(h,t)} \tag{4.9}$$

Note that this distribution is only valid within a 3 hour sea state, and is ultimately a function of H_s and T_p.

The standard deviation $\sigma_x(h,t)$, and zero-up crossing frequency $\nu^+_{x,0}(h,t)$ are functions of the spectral moments, which are found from integration of the spectrum.

$$\sigma_x^2(h,t) = m_x^{(0)}(h,t) \tag{4.10}$$

$$\nu^+_{x,0}(h,t) = \frac{1}{2\pi}\sqrt{\frac{m_x^{(2)}(h,t)}{m_x^{(0)}(h,t)}} \tag{4.11}$$

The spectral moments are defined as:

$$m_x^{(j)}(h,t) = \int_0^\infty \omega^j S_x(\omega;h,t)d\omega \tag{4.12}$$

$\eta_{3h}(h,t)$ is the expected number of global maxima in the sea state. It is defined as:

$$\eta_{3h}(h,t) = 10800 \cdot \nu^+_{\Gamma,0}(h,t) \tag{4.13}$$

10800 is the number of seconds in 3 hours.

Undertaking the analysis in frequency domain is less time consuming and requires less computational resources. The central assumption here is that there is a linear relation between wave amplitude and load amplitude, as well as load amplitude and response amplitude. A system with these properties are called a linear system. While this is not always the case for offshore systems, by assuming that it is valid, it is possible to get good results for both fatigue calculations, and dynamic analysis of large volume structures, such as semi-submersibles[13].

Time domain

For a linear mechanical model experiencing nonlinear loads, e.g. higher order wave loads, one should solve the problem in time domain. By undertaking multiple time domain simulations of the structure subjected to irregular waves, using random seeds, one can obtain a set of realizations, and then fit a distribution to this set. Similarly to frequency domain a Gumbel model is usually the best fit. One way to fit the probability model to the sample is using the method of moments. The Gumbel distribution function can be given on the following form:

$$F_{X_{3h}}(x) = exp\{-exp\{-\frac{x-\alpha}{\beta}\}\} \tag{4.14}$$

in this case x is the global maxima.

Estimates of the parameters is given as:

$$\hat{\beta} = 0.07797 S_Y \qquad \& \qquad \hat{\alpha} = \bar{y} - 0.57722\hat{\beta} \tag{4.15}$$

where S_Y and $\bar{y}$ are respectively, the standard deviation and mean value of the sample.

The validity of this model depends on the size of the sample the distribution is fitted to. Haver[10] recommends a minimum sample size of 20, but a higher number is preferable.

The Gumbell distribution has been found to give good results when fitted to the distribution of extreme responses. This can then be done for various combinations of H_s and T_p, resulting in a dataset which a continuous function can be fitted to. In this way the short term distribution as a function of the sea state parameters is obtained. However this process can be both time and resource consuming. To get a good fit for the distribution model, it is necessary to undertake a large number of time domain simulations.

Having found both the long term distribution of the sea state parameters, and the short term distribution of the 3-hour maximum, either using frequency or time domain, the long term distribution of the 3-hour maximum is found according to Equation 4.4. The q-probability response is then found by solving Equation 4.16 for x_q:

$$1 - F_{X_{3h}}(x_q) = \frac{q}{m_{3h}} \tag{4.16}$$

m_{3h} is the number of three hour sea states per year, e.g. $m_{3h} = 2920$ if one uses all sea states, when determining the long term distribution of the sea state parameters.

Long term stochastic analysis is the preferred method when the structural response is close to linearly related to the wave process. It is then easy to establish a short term distribution of the characteristic response. When this is not the case it is more costly to establish the short term distribution and other methods are preferable.

Contour line method

Another method commonly used is the contour line method. Having determined the long term distribution of the sea state parameters, it is possible to find the combinations of H_s and T_p that will have a q-annual probability of occurring. This set of combinations will fall on on a contour line. The most unfavourable sea state along this contour line should give us the largest response. Further, only a few of the sea states along the contour line is likely to be the most unfavorable sea state. Therefore the number of sea states that must be considered are considerably reduced.

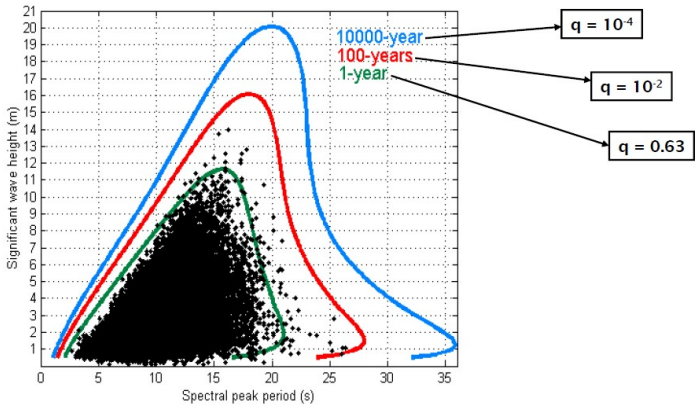

Figure 4.1: Example of q-probability contours[10]

The contour line method will most frequently be used in association with time domain analysis. In order to determine the worst sea state, time domain simulations of the structure in irregular sea should be run. The worst sea state should then reveal itself as the one which gives the largest response. One should then run more simulations for that sea state, and use the results to establish a probability distribution for the largest response.

An adequate estimate of the q-probability response is then found by solving:

$$F_{X_{3h}\backslash H_s T_p}(x_\alpha \backslash h_q, t_q) = \alpha \tag{4.17}$$

where h_q and t_q are the sea state parameters defining the worst sea state along the q-probability contour line. α is a percentile of the three hour extreme value distribution that based on experience yields a reasonable estimate of the q-probability response. $\alpha = 0.9$ is the recommended value when finding the 10^{-2}-probability response.

The contour line method is the preferred approach when the problem is quite complex, e.g. when numerical calculations or model tests are necessary to solve the equation of motion.

4.3 Wave spectra

4.3.1 Irregular waves

Irregular waves can be taken to consist of a sum of regular waves, with different amplitudes, frequencies and phase angles. The distribution of these regular waves can be described using a wave spectrum. This assumes that the sea can be described as a stationary stochastic process, that the wave elevation has a normal distribution with zero mean and variance, and that the process is ergodic.

The surface elevation of an irregular sea state is given as :

$$\zeta(x,t) = \sum_{j=1}^{n} \zeta_{aj} cos(\omega_j t - k_j x + \epsilon_j) \tag{4.18}$$

Here long crested head waves are assumed. ϵ_j is a phase angle, modeled as a stochastic variable uniformly distributed between 0 and 2π. k_j is the wave number dependent on ω_j.

Equation 4.18 shows how the irregular surface elevation is calculated by superposition of many regular waves. The randomness of the surface elevation is expressed in the phase angle.

The regular wave amplitude $\zeta_{aj} =$ is calculated from the spectrum as:

$$\zeta_{aj} = \sqrt{\int_{\omega_{l,j}}^{\omega_{u,j}} S_\zeta(\omega) d\omega} \tag{4.19}$$

where $\omega_{u,j}$ and $\omega_{l,j}$ are the upper and lower limits of then integral based on how the spectrum is discretized.

4.3.2 The JONSWAP spectrum

The JONSWAP spectrum ("Joint North Sea Wave Project") is a standardized wave spectrum based on measurements in the south-east of the north sea, and as such is much used when modeling sea states in the north sea. The spectrum is special, in that it has a rather sharp peak compared to the Pierson-Moskovitch spectrum, another frequently used spectrum. The measurements the spectrum is based on comes from an area of the north sea with relatively shallow water and also quite close to shore.
The aim when establishing the spectrum was to describe a not fully developed sea state i.e. a sea state where the wind has not been blowing long enough for the sea state to stabilize[13]. It should be well suited to be used in analysis of Havfarm 1 given the location close to shore.

The Jonswap spectrum as a function of wave frequency ω is given as [8]:

$$S(\omega) = 155 \frac{H_{\frac{1}{3}}}{T_1^4 \omega^5} exp(\frac{-944}{T_1^4 \omega^4})(3.3)^Y \tag{4.20}$$

where

$$Y = exp(-(\frac{0.191\omega T_1 - 1}{2^{\frac{1}{2}}\sigma})^2)$$

and

$$\begin{aligned} \sigma &= 0.07 \; for \; \omega \leq 5.24/T_1 \\ &= 0.09 \; for \; \omega > 5.24/T_1 \end{aligned}$$

$H_{\frac{1}{3}}$ is the significant waveheight, defines as the mean of the one third highest waves. T_1 is a mean wave period connected to the peak spectral period T_p, by the relation:

$$T_1 = 0.0834 T_p \tag{4.21}$$

According to DNVGl-RP-C205 the JONSWAP spectrum is expected to be a reasonable model when in the range[7]:

$$3.6 < \frac{T_p}{\sqrt{H_S}} < 5 \tag{4.22}$$

for larger values than 5 the Pierson-Moskowitz spectrum should be used. Also in this range it is recommended that the value shape parameter γ is taken as:

$$\gamma = exp(5.75 - 1.15 \frac{T_p}{\sqrt{H_s}}) \tag{4.23}$$

however the average value $\gamma = 3.3$ has been used here.

There is also a steepness criterion. The wave steepness can be expresssed as:

$$S_p = \frac{2\pi}{g}\frac{H_s}{T_p^2} \tag{4.24}$$

where g is the gravitational constant. The limiting value of S_p may be taken as:

$$S_p = 1/15 \; for \; T_p \leq 8s$$
$$S_p = 1/25 \; for \; T_p \geq 15s$$

and interpolated linearly between the boundaries.

4.4 Damped eigenfrequency

A common way to describe damping in a system is the damping ratio ξ defined as[13]:

$$\xi = \frac{c}{c_{cr}} = \frac{c}{2m\omega_0} \tag{4.25}$$

where c is the damping coefficient in the equation of motion, m is the mass and ω_0 is the natural frequency.

When the damping ratio is less than one, $\xi < 1$, the damping is said to be sub-critical. This is the case for most real structures. Based on this, the concept of the damped eigenfrequency is introduced:

$$\omega_d = \omega_0\sqrt{1-\xi^2} \tag{4.26}$$

This can be expressed as the damped eigenperiod:

$$T_d = \frac{2\pi}{\omega_0\sqrt{1-\xi^2}} \tag{4.27}$$

Larsen et al.[13] shows how the structure will oscillate with this period, when subjected to an impulse load. Therefore resonance will be found at this period, not the natural period. However, in most cases the difference between the two periods are negligible.

Chapter 5

Vegard Holen's Havfarm 1 model

5.1 USFOS

The model of Havfarm 1 was made for use with the structural analysis program USFOS. The program is developed and maintained by SINTEF in association with NTNU, and is designed for non-linear static and dynamic analysis of space frame structures. USFOS was originally made to study bottom fastened offshore structures, but has also been applied to both floating structures, as well as structures on land. The program uses a very coarse finite element modeling of the structure, but still obtain results with excellent accuracy. It is especially well suited for collapse analyses and accidental load analyses of fixed offshore structures, intact or damaged[21].

Since USFOS was originally meant for bottom fixed structures there are some missing features that make the analysis somewhat more difficult. In addition it can be said to be somewhat bare bones. While other structural analysis programs may come with an inbuilt modeling tool or many post-processing capabilities, USFOS is more limited. However it does come with a graphical user interface allowing the user to observe the model and verify the results. The program also delivers good results, depending on user input. The program is very suited for ULS analysis of structures.

USFOS has been used in conjunction with scripting in python, in order to undertake stochastic analysis in both frequency and time domain. This includes preparing the input files by manipulating text files, initiating the analysis, running multiple instances of USFOS simultaneously, retrieving the results and processing the results.

5.2 Holen's Model

In his Thesis, Holen gives a comprehensive account of the modeling of the Havfarm. A summary of his modelling decisions will be given here.
The main structure consists of 4 submerged longitudinal pontoons, and two longitudinal beams, connected with seven vertical columns on each side. Both pontoons and columns add to the buoyancy and some contain ballast tanks. The middle and bottom pontoon is connected with 24 circular braces on each side. The two sides are connected with seven transverse beams at both top and bottom. These are stiffened with 12 cross braces at the top.

5.2.1 Changes to the final concept

The design of Holen's model is quite different from the design of the final structure, as can be seen by comparing figure 5.1 and 5.2. At the time, the design process of the fish farm was still

at an early stage. Holen states in his master thesis[11] that: "The model is based on design drawings (General Arrangement) supplied by NSK Ship Design, when deatils of the design have been found lacking, sound engineering judgement have been employed, especially in regard to weight distribution, mooring lines and net pens."

The overall dimensions of the structure has changed slightly in the final design. The dimensions of the model, and the overall dimensions of the finished structure are given in Table 5.1.

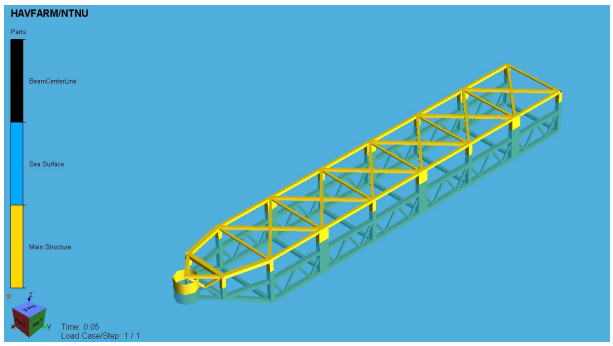

Figure 5.1: Holens model shown in USFOS GUI

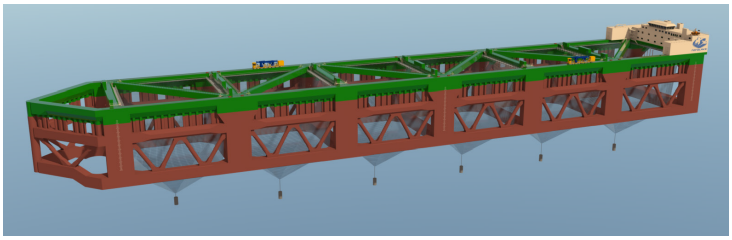

Figure 5.2: Final concept[17]

Dimension	Model	Finished structure
Length Pen Section$[m]$	336	-
LoA$[m]$	396	385
Height$[m]$	40	37.75
Width$[m]$	60	59.5
Pen depth$[m]$	63	56
Operation Draft$[m]$	30	30

Table 5.1: Model dimensions

A stark difference between the two designs can be seen in the bow. Holen's bow design is based on counteracting the mooring line forces. It consists mainly of a large buoyancy element connected to the rest of the structure with a front that narrows towards the element. Initially Holen used a catenary equation to model the mooring forces. This resulted in a large downward force in the bow. In order to counteract the force, the large buoyancy element was introduced. However using a catenary equation led to instability in the numerical calculations, which resulted in Holen replacing it with a spring model instead. This removed the large downward force, but instead of changing the bow design, Holen left it as it was, most likely due to time constraints. The final structure has a shorter bow, still with a circular element in front. The two front pontoons are bent.

Another point is the choice of cross-sectional properties. Since there were no drawings of the stiffeners or cross-sections the cross-sectional properties had to be based on estimates of the final steel weight given by the design company. The stiffeners are therefore modeled as smeared and the thickness of the structural elements tries to achieve expected steel weight. The cross-sectional properties are given in Table 5.2

Element	Height	Width	Diameter	Side thickness	Top thickness
Bottom pontoon	3.0	4.0	-	0.091	0.114
Middle pontoon	3.0	4.0	-	0.091	0.114
Top pontoon	2.5	2.5	-	0.029	0.033
Vertical Column (small)	4.0	4.0	-	0.030	0.030
Vertical Column (large)	4.0	10.0	-	0.030	0.030
Horizontal Bottom Brace	2.5	3.0	-	0.037	0.049
Horizontal Top Brace	1.0	2.5	-	0.032	0.032
Cross Braces Top	2.5	2.5	-	0.024	0.032
Braces sides	-	-	2.5	0.035	-

Table 5.2: Cross section dimensions [m]

The primary structure is modeled using NV-36 steel, and the properties are given in Table 5.3

Property	Symbol	Value	Unit
Young's modulus	E	210	GPa
Poisson's ratio	ν	0.3	-
Yield Strength	σ_y	355	MPa
Density	ρ_s	7850	kg/m^3

Table 5.3: Material properties

Another large change is that of the crossbraces. They have been removed and instead there are one diagonal brace placed in a snaking pattern along the top. One can assume that the use of 2 braces added an unnecessary amount of stiffness and unwanted weight.

The final structure is also outfitted with a "skirt" between the longitudinal beam and pontoon. The skirts function is to affect wave attenuation, in order to better the conditions of the fish in the pens.

5.2.2 Mass distribution

The goal was to achieve a model with a stable draught close to 30 meters. In order to do so, in addition to the steel weight, point loads representing ballast water was used. Holen notes that "To achieve a correct draught it has been chosen to fill the bottom pontoons with ballast water, this is probably not a realistic scenario." The loads was applied asymmetrically in order to counter act the large buoyancy element in the bow. The choice of using such a large buoyancy element and asymmetric weight is somewhat questionable. Holen states himself that this made it difficult to establish a stable draft without cyclic pitch motion.

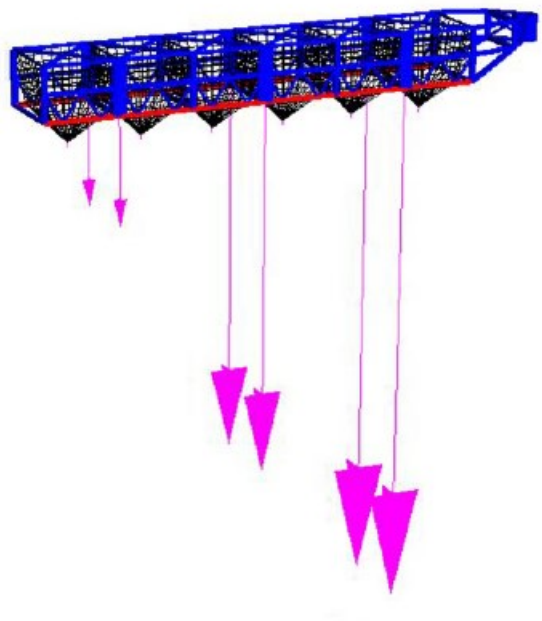

Figure 5.3: Nodal masses and fill ratio of bottom pontoon[11]

Property	Mass	Unit
Steel mass	31 270	tonnes
Total nodal mass	2 200	tonnes
Net Mass	824	tonnes
Total mass	34 294	tonnes

Table 5.4: Mass distribution

5.2.3 Loading

Hydrodynamic wave loading is modelled using Morrison's equation, which is widely used to calculate the forces on circular cylindrical structural members. The equation gives the force (dF) on a horizontal strip (dz) of a vertical rigid circular cylinder as[8]:

$$dF = \rho_w \frac{\pi D^2}{4} dz C_M a_1 + \frac{\rho_w}{2} C_D D dz |u| u \tag{5.1}$$

Positive force direction is in the wave propagation direction. ρ_w is the density of water, D the cylinder diameter, u and a_1 the undisturbed horizontal water particle velocity and acceleration at the midpoint of the strip. C_M and C_D are empirical mass and drag coefficients. Figure 5.4 shows under what circumstances the different terms are important.

The form of the equation shown in Equation 5.1 assumes a static body. A modified version accounting for the motion of the cylinder can be written as:

$$dF = \frac{\rho_w}{2} C_D D dz |u - \dot{\eta}_1| (u - \dot{\eta}_1) + \rho_w C_M \frac{\pi D^2}{4} dz a_1 - \rho_w (C_M - 1) \frac{\pi D^2}{4} dz \ddot{\eta}_1 \tag{5.2}$$

The dot means time derivative and η is the horizontal position of the horizontal strip. Here C_M and C_D are not necessarily the same as in Equation 5.1.
The mass and drag coefficients must be estimated empirically. The factors that most impact the values of the coefficients are:

1. The Reynolds number, $Re = \frac{UD}{\nu}$
2. The Keulegan-Carpenter number, $KC = \frac{UT}{D}$
3. Roughness number, $\frac{k}{D}$

k is a measure of the surface roughness, T is the wave period, U the characteristic free stream velocity and ν the kinematic viscosity coefficient.

Holen made his choice of coefficients based on empirically established coefficients found in DNV RP-C205[7] and in NORSOK N-003[19]. They are given in Table 5.5

Cross-section	C_d	C_M
Box sections	2.2	1.68
Pipes	1.05	1.2

Table 5.5: Drag and mass coefficients

When determining what loads will dominate the structural response it is important to consider the size of the structure relative to the wave height H and wavelength λ. Figure 5.4 shows a rough categorization for when different load components are of importance. According to Nordlaks the significant wave height used in design is 6 meters[17]. Taking the characteristic value for the structural dimension, D, to be around 4 meters it is safe to say the structure will be mostly affected by mass forces. An exception is the net where viscous forces will be significant. Wave diffraction can be said to be of little importance.

5.2.4 Damping

Langen et al. defines damping as follows:

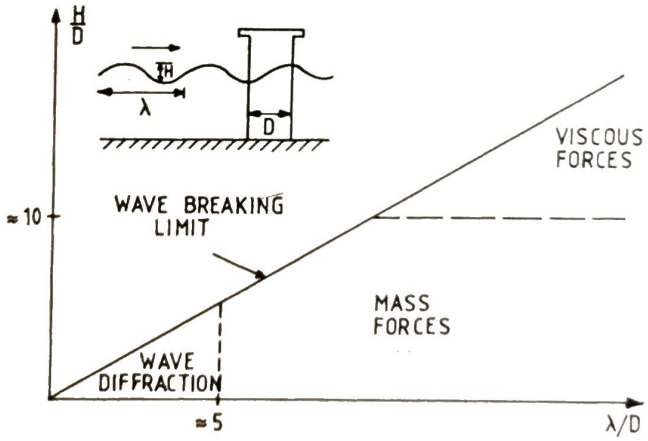

Figure 5.4: The relative importance of wave forces as a function of wave and structure dimensions.[8]

> Damping designates the ability of a structure to dissipate kinetic energy i.e. to transform it into other types of energy such as heat or radiation (of water waves, sound waves etc.). For a real vibration system there will always be damping present so that the kinetic energy of the system will decrease if no external energy is supplied.[12]

Damping of structures in water can be split in two categories, Hydrodynamic damping and structural damping, where both contribute to the total damping of the structure. Hydrodynamic damping can be said to be a result of the interaction between the water and the structure. Structural damping is related to the internal friction of the material as it bends or stretches. As damping is quite complex and usually hard to model correctly, simplified models have been introduced.

Hydrodynamic damping

Hydrodynamic damping can usually be assumed to consists of two parts. The first part is connected to the creation of waves generated by the moving structure. This component is proportional to the velocity and can be described using a linear viscous model. The second part is often given the name drag damping, and is connected to vortex shedding and other viscous effects. This term is proportional to square of the relative velocity between the structure and water particles. The magnitude of the terms depend on a variety of factors. By default USFOS does not account for the relative velocity between the structure and water particles. In order to do so one must make use of the REL_VELO command.

Holen determined that the damping will be dominated by drag forces calculated using Morison's equation. The linear viscous model was therefore neglected.

Structural damping

Structural damping can be described using a so called "Hysterisis curve" which is obtained when the material is subjected to cyclic loading. An example of such a curve is given in Figure 5.5. The area within the curve represents the energy loss per unit of volume for one load cycle. The magnitude of the damping coefficient is found from this curve.

The structural damping will only be a small contributor to the total damping and not affect the global response. However, when considering the local response of individual members it is

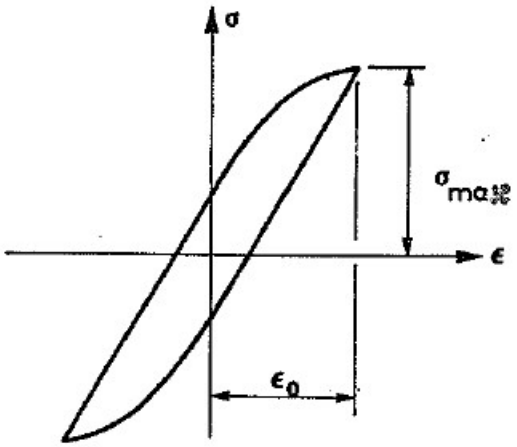

Figure 5.5: Example of a hysterisis curve[12].

of interest. One way to model the structural damping is the use of Rayleigh or proportional damping. The damping is assumed to consist of two term, one proportional to the structural stiffness and one proportional to the mass.

$$\mathbf{C} = \alpha_1 \mathbf{M} + \alpha_2 \mathbf{K} \tag{5.3}$$

$\mathbf{C}$ is the damping matrix, $\mathbf{M}$ the mass matrix and $\mathbf{K}$ the stiffness matrix. α_1 and α_2 are the damping parameters and can be found if the damping ratios, λ for two different response frequencies, ω are known. Typical values for damping ratios in steel structures are in the range of 0.5%-0.8% according to Langen et al.[12]. As the structural damping is not known these values are used and the damping parameters are given in Table 5.6

Parameter	Value
ω_1	2.0944
ω_2	0.0628
λ_1	0.05
λ_2	0.05
α_1	0.0061
α_2	0.0464

Table 5.6: Structural damping parameters

5.2.5 Mooring

In order to avoid drift off of the structure when simulating regular waves and current, the structure must be moored. The mooring line is modeled as a linear spring connected to the bow and sea bottom, with stiffness in the global x-direction. Holen states that originally a more realistic catenary model was used, but due to numerical errors it was replaced by a linear spring model. The spring force is given by Equation 5.4

$$F = k * X \tag{5.4}$$

The value of the spring coefficient k is $400kN/m$. X is the displacement.

5.2.6 Net pens

Vegard Holen used a lot of time and effort in producing his finite element model, and a significant portion was spent on the modelling of the net pens. For a thorough explanation of the modeling decisions the author recommends reading Holen's thesis.
Typically, the net of a fish farm will consists tens of millions of twines. Such an amount of complexity is not feasible to model using modern computer software and therefore a simplified representation is used. There are six net pens in the model, each consisting of a trapezoidal prism forming the top and a pyramid forming the bottom. The main objective in modeling the net pens, was that the forces should transfer to the load carrying structure so that they contribute to the global behaviour. The behavior of the net pens and their deformation may therefore not represent reality.

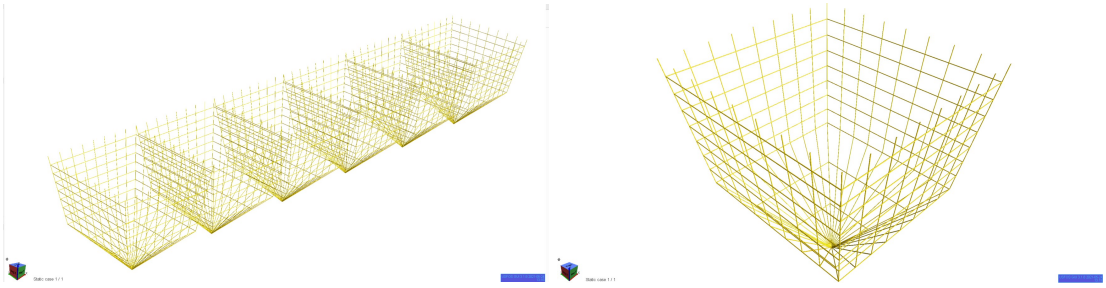

(a) All six net pens *(b) Single net pen*

Figure 5.6: The modelled net pens

Dimension	Value
Top width$[m]$	60
Top length$[m]$	56
Depth top section$[m]$	38
Pyramid width$[m]$	48
Pyramid length$[m]$	44
Pyramid depth$[m]$	25
Total depth$[m]$	63
Single net pen volume$[m^3]$	104 544

Table 5.7: Net pen dimensions

The net is modeled using tubular elements and are close to solid. They are modeled like this and with increased stiffness and dimensions in order to avoid computational errors. USFOS will terminate a simulation if it experiences to large incremental rotations in any part of the structure. The net is prone to experience this, and through a large amount of trial and error the present dimension and properties were determined by Holen. Though the stiffness of the net is increased the contribution to the overall stiffness of the structure is negligible. An alternative to changing the stiffness would have been to reduce the step length of the simulation. This however, would have led to an exponential increase in computation time.

Holen made used of a Modified Morison model when calculating the loads on the net pens. The theory behind this model and implementation of it can be found in Bore et al.(2017)[1].

5.2.7 Comments on the model

Holens model seems to give realistic results, however the design is not optimal. The modeling of the bow is not ideal, and compared to the final design seems unreasonable. The use of a large buoyancy element introduces unnecessary asymmetry which had to be rectified by asymmetrical distribution of the mass. This leads to sub-optimal behaviour, which can be seen in the results of both the decay test and when subjected to regular waves. However, Holen lacked information when creating his model and should not be blamed for creating a sub-optimal model. In fact, it has been a boon to already have a ready made model to work with.

Chapter 6

Analyses of the model

6.1 Preliminary studies

Some simple introductory analyses was carried out in order to get familiar with both software and modeling, as part of the project thesis. This is told here, as some of the findings from the project thesis was used in the master thesis. In the following the water depth is taken to be 160 m deep.

6.1.1 Decay test

As previously discussed, since Havfarm 1 is a floating structure the effects of dynamics will play a large role in the response. It is therefore necessary to obtain the natural periods of the structure in several motions. If the structure were to be put under oscillating loads with periods in close vicinity of the natural periods, resonance would occur. Resonance is characterized by very large motions, caused by periodic loads with a period close the mechanical systems natural period. In designing a structure one therefore wants make sure the natural periods lie outside of the typical excitation range of the most prominent loads, in this case waves. For semi-submersibles, a type of structure similar to Havfarm 1, resonance is avoided in heave when the natural period is upwards of 20 seconds.

Since USFOS originally was designed for the analysis of bottom fixed structures, it does not include any "out of the box" routine for calculating the natural periods of rigid body motions. There are however methods for acquiring these the natural periods.

A decay tests consist of exciting the structure with an impulse load. The load causes the structure to move and it will oscillate with it's own natural period. The load must excite the structure in the relevant mode of response. Relevant modes in this case are heave and pitch. The motion in surge, sway and yaw will be governed by the mooring stiffness and is not of large concern. Since the structure is weather waning around the mooring point, waves will mostly be propagating from the bow and backwards. Roll is therefore of little concern as it is excited by transversely propagating waves.

According to Faltinsen[8] the natural period in heave can be found by:

$$T_{n3} = 2\pi\sqrt{\frac{M + A_3}{\rho_w g A_w}} \tag{6.1}$$

M is the total mass of the structure, A_3 the added mass in heave and A_w the total waterline area. Equation 6.1 shows that a change in the total mass of the structure has a big impact on

the natural heave period.

Note that it is assumed that the body motions are uncoupled, which in reality is not true due to the asymmetry of the structure. Even though this assumption does not hold, it should be possible to obtain usable estimates of the natural period.

In order to excite heave motion, the structure was lifted 10 meters up out of the water. The structure is subjected to regular waves, but with an insignificant wave height. This is due to the way USFOS models water, Hydrodynamic properties are connected to waves and current in USFOS. The structure is not moored in this simulation. When the simulation starts the structures falls and begins bobbing up and down. The motion slowly dies out as the simulation goes on. The heave response can then be expressed in a dynamic plot by USFOS, as a function of frequency. The frequency connected to the largest excitation is the natural frequency. In actuality the observed frequency is the damped natural frequency, however in most practical case the difference between the undamped and damped natural frequency is negligible.[13]

When finding the natural frequency in pitch a moment is applied to the structure. Two nodal moments are applied on each side of the middle cross beam, acting in positive pitch direction. The moments are applied as an impulse going from zero to 1 GNm over the course of 10 seconds, and then lowered to 0 over one second.

The motion is measured at a node close to the longitudinal center of the structure. The position of the node is shown in Figure 6.1. Pitch should ideally be measured at the center of rotation, however the exact center has not been used as it is complicated to establish its location.

Note that in this analysis the model is without the net pens.

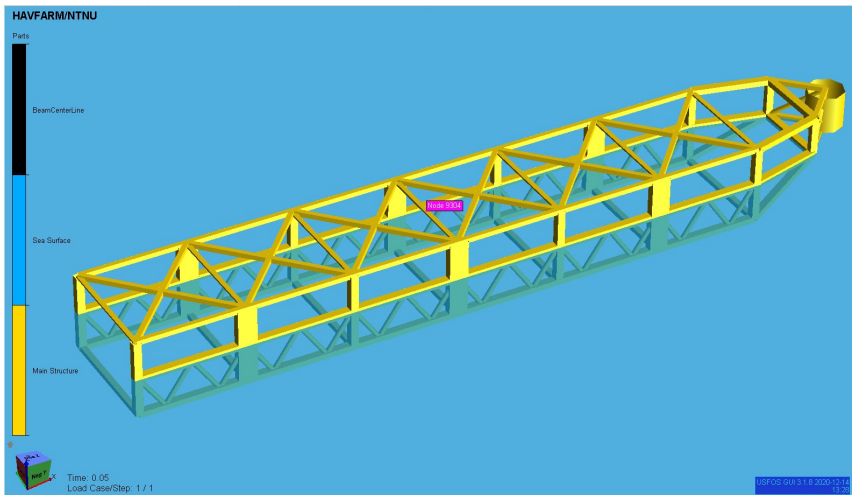

Figure 6.1: Location of the measuring node

Results

Figure 6.2 shows the heave response of node 9304 as a function of frequency. The heave response is in meters, while the frequency is in Hz. Node 9304 is located close to the middle of the structure. The peak is found at 0.0427 Hz which corresponds to a period of approximately 23.4 seconds. There also seems to be small peak at 0.0854 Hz.

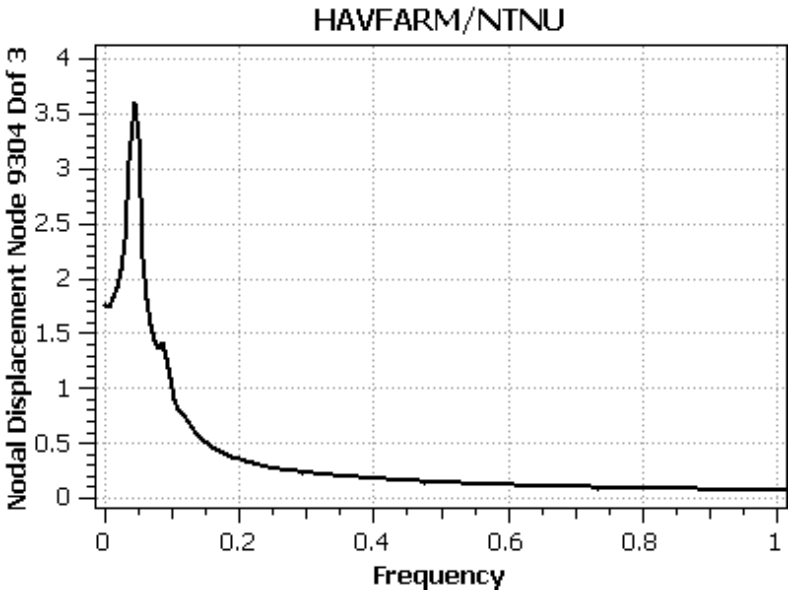

Figure 6.2: Vertical displacement as a function of frequency

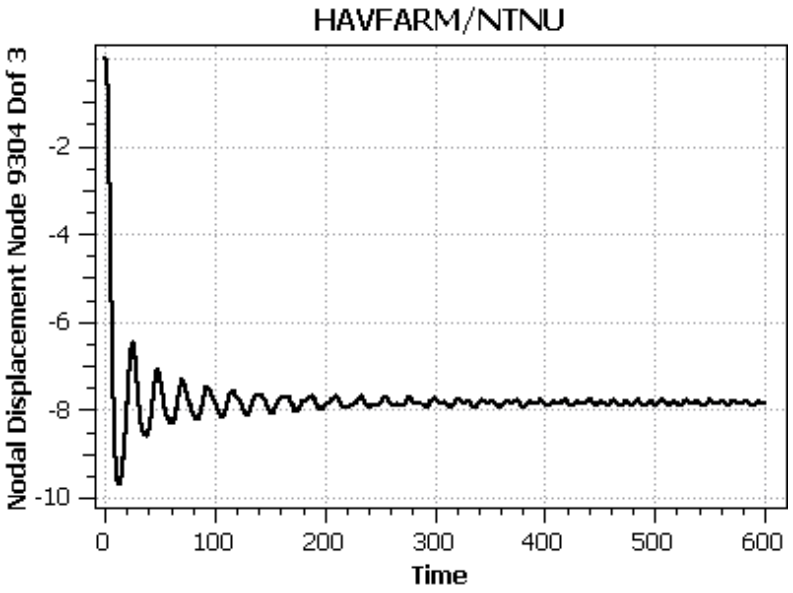

Figure 6.3: Vertical displacement history

Figure 6.4 shows the rotation of node 9304 in pitch as a function of the frequency. The figure shows two peaks. Figure 6.5 shows the rotation over time, and from the plot one can observe the response contains multiple frequencies. Compared with the heave response shown in Figure 6.3 the response in pitch is irregular.

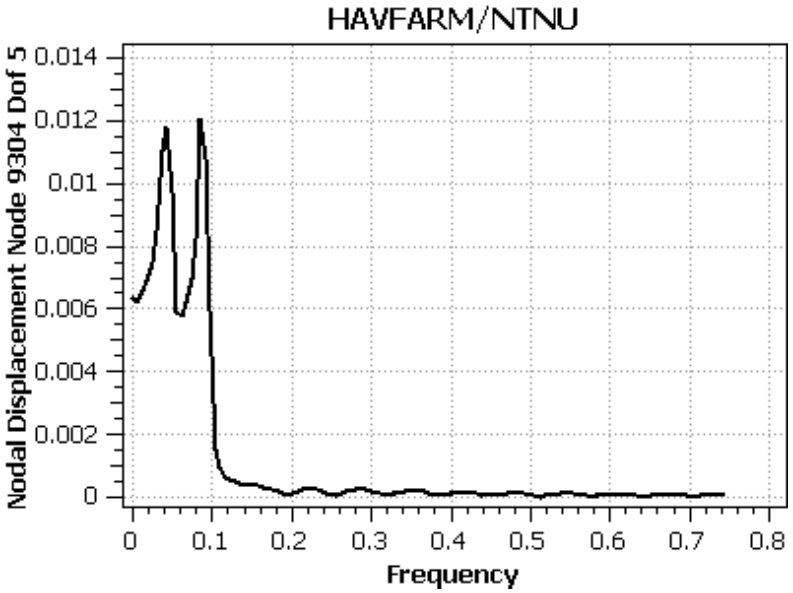

Figure 6.4: Rotation displacement as a function of frequency

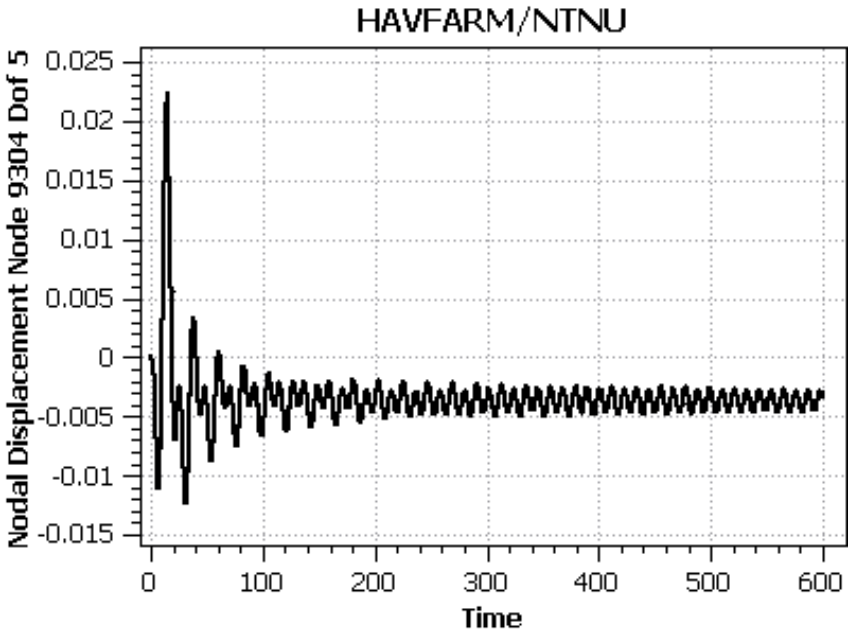

Figure 6.5: Rotation over time

Peak	Frequency [Hz]	Period [s]
1	0.0427	23.4
2	0.0854	11.7

Table 6.1: The pitch results of the decay test.

Discussion

Figure 6.2 shows one large peak at 0.0427 Hz, and a small peak found at 0.0854 Hz. These frequencies corresponds to peaks in Figure 6.4. The presence of two peaks is an indication of coupling of the heave and pitch motion. Due to the asymmetry between the bow and aft when the structure rises, the buoyancy and mass leads to the ship pitching. This is why we find peaks corresponding to the same frequencies in both plots.

The first peak in Figure 6.2 is larger than the second suggesting that wave loads with a period of 23.4 seconds will excite heave motion more than those with a period of 11.7 seconds. Pitch motion it seems is excited equally. The first natural period falls outside the typical excitation range of waves, from 4-20 seconds, which is positive. The second period however falls in the middle of the range and waves with this period is likely to occur. However, the value of the natural periods should be highly dependent on the shape of the bow, and as noted previously the design Holen opted for is very different from that of the final structure.

If we assume deep sea, which is reasonable with a water depth of 160 meters, we have that:

$$\omega^2 = k \cdot g \tag{6.2}$$

Equation 6.2 is known as the deep water dispersion relation[8] and shows the relation between the wave frequency ω given in rad/s, the wave number k and the gravitational constant g. The wave number is related to the wavelength λ by the following relation:

$$\lambda = \frac{2\pi}{k} \tag{6.3}$$

Using this it is possible to calculate wavelengths corresponding to the two natural frequencies. This is shown in Table 6.2. The first frequency corresponds to a wavelength which is in the order of twice the length of the fish farm.

Frequency [Hz]	ω	Wavelength [m]
0.0427	0.26683	856.3
0.0854	0.53658	214.1

Table 6.2: Wavelengths corresponding to the natural frequencies.

Notice also that the first frequency, 0.0427 is half of the second frequency, 0.0854. This also means that wavelength corresponding to the first frequency is 4 times the length of the wave corresponding to the second frequency.

Figure 6.6 shows the structure subjected to wave with a period of 23.4 seconds. In the plot the the peak is at the center of the structure and the structure is moving upwards. This means the largest positive buoyancy force is being experienced as the structure is moving upwards. If the wave length were shorter the force would be that large since there would be an air gap at point along the structure. It makes sense that the natural period in heave corresponds to this wavelength.

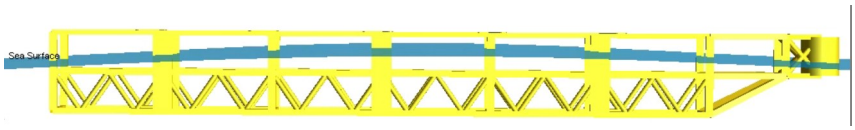

Figure 6.6: Wave corresponding to a period of 23.4 seconds

6.2 Investigating model behaviour

A stated goal was to conduct analysis of the fish farm in regular and irregular waves and eventually estimate the characteristic response e.g. by means of the contour line method. In order to do this 2 initial goals were set: 1. Evaluate the behaviour of the structure in regular waves, for both very small and small wave heights. 2. Establish a transfer function in order to conduct stochastic analysis in frequency domain.

The choice of response has fallen on heave motion of the structure. The reasoning behind using a rigid body motion and not the stress in a limb is twofold: First, the structure will house crew, and in order to ensure safe working conditions the rigid body motions must not be to large. The importance of the different motions has been discussed previously. Second, the dimensions of the model members are not representative of the finished structure. Neither is the dimensions of the bow. Therefore the stresses in the members are not representative. Further, Holen found in his master thesis that the structural members are in fact over-dimensioned, with respect to yield utilization.

6.2.1 Establishing a transfer function

In the preliminary work the Eigenperiods were found using numerical decay tests. Now the objective is to establish a transfer function of the characteristic responses. A transfer function or similarly a Response Amplitude operator(RAO) is a mathematical expression defining the linear relationship between a regular wave and the structural response as a function of frequency/period. This is represented as a plot of the response for varying frequencies/periods.

From theory it is expected to find a large amplification close to the eigenperiods found in the preliminary study. For larger periods the RAO should go to 1[13]. This can be explained intuitively, by the fact that waves with larger periods are also longer, and when the wavelength is much larger than the length of the structure, the structure moves with the wave.
For smaller periods the excitation should approach zero. When the periods are small so too is the wavelength. In reality so too should the wave height since the waves cannot be to step or they will break. When there are many small wave peaks and troughs along the length of the structure, the sum force is zero. Therefore the RAO goes to zero for small periods.

Initial simulations

In order to obtain the transfer function, several time domain simulations is run in USFOS where the structure is subjected to regular waves. In the initial simulations the model was also subjected to a small current and only the model without net was used.

The structure is subjected to regular airy waves and by keeping the wave amplitude small, nonlinear effects should be negligible. The waves have an amplitude of .1 m and the period varies from 2 to 20 seconds, with steps of .9 second. Each simulation was ran for 600 seconds. Using python scripting multiple instances of USFOS simulations can be run simultaneously,

saving time. In this analysis only heave motion was measured, and it was measured using the motion of Node 4024 located app. at the longitudinal midpoint of the structure. The structure is not front-aft symmetric and the longitudinal rotational center is hard to establish. However little effect of the pitch motion should be experienced in this point.

In the first run of this analysis the first 100 seconds of the response was discarded. The analysis yielded the following figure:

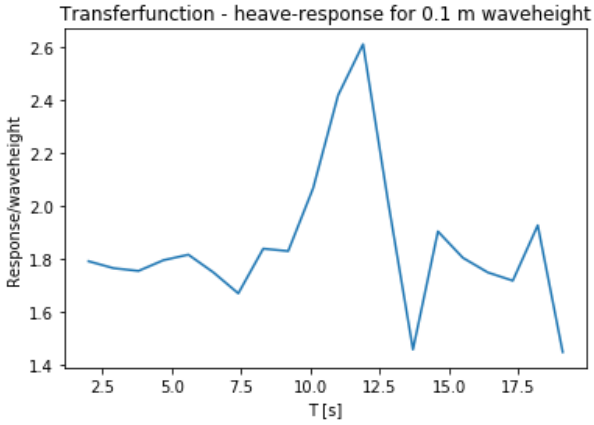

Figure 6.7: Initial transfer function

Figure 6.7 shows something resembling a transfer function or RAO. There is the distinct peek close to the previously established natural period. However the amplification is very large and very sporadic. For small periods the amplification is way too large. This is likely due to the presence of transient motion that has not died out yet. The transient motion stems from the structure not being in equilibrium at the start of the simulation.

Taking only the data after 200 seconds yields a different plot. This is shown in Figure 6.8.

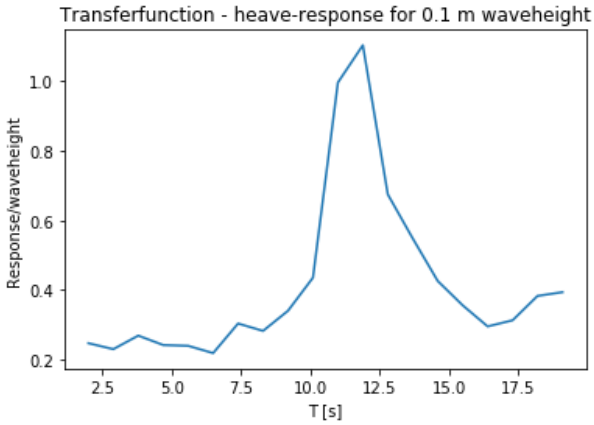

Figure 6.8: Second transfer function

This figure shows something more akin to what is expected from an RAO. The amplification is 1.1 when the period is 11.9, which is not a lot. This could mean there is a lot of hydrodynamic damping involved. The prelimenary studies yielded an eigenperiod at 11.7 which is close to the peak found in both figure 6.7 and 6.8. It can also be seen in Figure 6.8 that the exitation is small for small periods. However it does not seem to converge to zero. This could be again attributed to transient motion.

In Figure 6.9 the time history of the heave motion is shown. One can observe that there is some small transient motion even after 200 seconds, although very faintly.

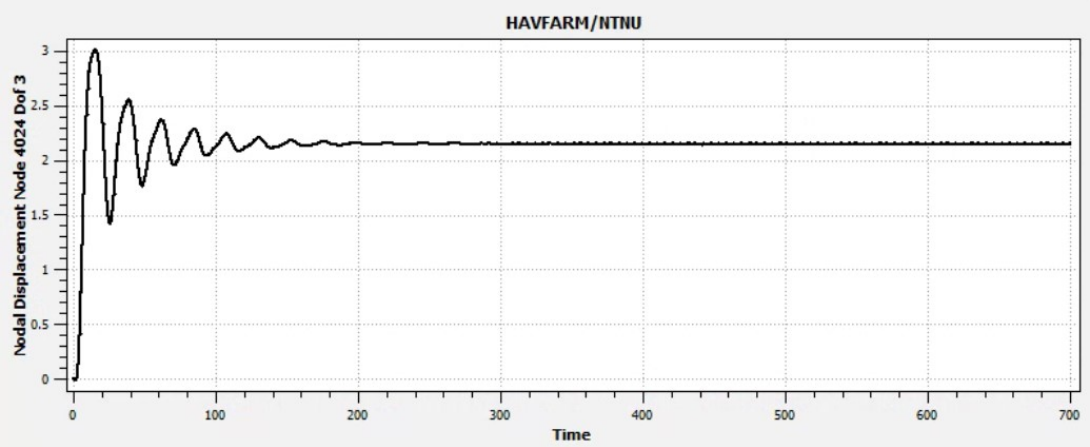

Figure 6.9: History plot of heave motion of the measuring node. $H = 0.1m$ and $T = 5.82s$

If possible the goal should be to eliminate all transient motion from the results. A new set of simulations were therefore run and this time removing the first 300 seconds from the results. In order to have enough data points an a additional 100 seconds were simulated, for a total of 700 seconds. In addition, the wave periods used in the simulations were changed in order to account for both natural periods observed in the preliminary studies. These are 11.7 seconds and 23.4 seconds. Every subsequent analysis ran 28 simulations with periods from 5 seconds to 27.18 seconds. This in sum means there was a large rise in required computational resources.

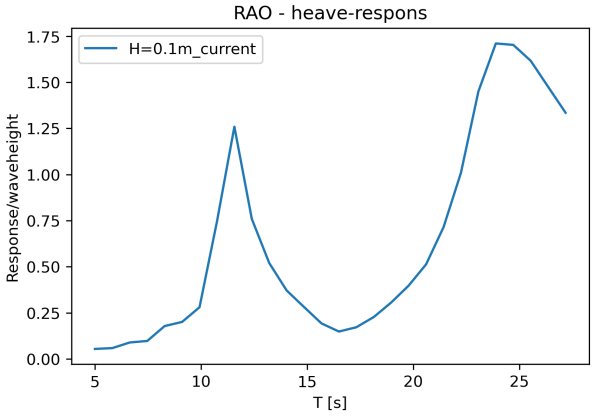

Figure 6.10: Third attempt at transfer function

Figure 6.10 shows the result of the third attempt at a transfer function. The transient motion seems to have been fully removed from the results. The amplification is only larger than one around the natural periods and it reduces to zero for the smallest periods. Both natural periods are represented in the plot and the largest amplification is found close to the largest period, the same as what was shown in the decay test. For the largest periods the amplification is more than one, but sinking.

As previously stated, the RAO should approach one for large periods. To check if it approaches zero a single simulation using a period of 40 seconds was run, yielding the following results:

Period [s]	Wave height [m]	Response height [m]	Amplification [-]
40	0.1	0.1125	1.125

Table 6.3: Results: Regular airy wave, period = 40 s

Table 6.3 shows that for large periods the ratio of the repsonse and waveheight is close to one. However there seems to be some amplification of the motion. A possible explanation is that there is some pitch motion adding to the motion of the measuring node.

6.2.2 Net-pen model

Having established the methodology and necessary scripts using the model without a net, a similar process was undergone with the net-pen model. The purpose was to test if the net pens have an effect on the response. From conversations with Ph.D. candidate Martin Slagstad he noted that when the designers conducted model testing there was little difference in the behaviour with or without the net pens. The net pens do add weight and create a larger area which is exposed to wave loads. However they are not very stiff and should not add to the heave motion of the structure, but more likely reduce the amplification due to viscous damping. At a waveheight of 0.1 m and an effective hydrodynamic diameter of 0.066 m for the net elements, the drag forces however should be negligible. Thus a reduced amplification is not necessarily to be expected, but there should not be a large change in amplification.

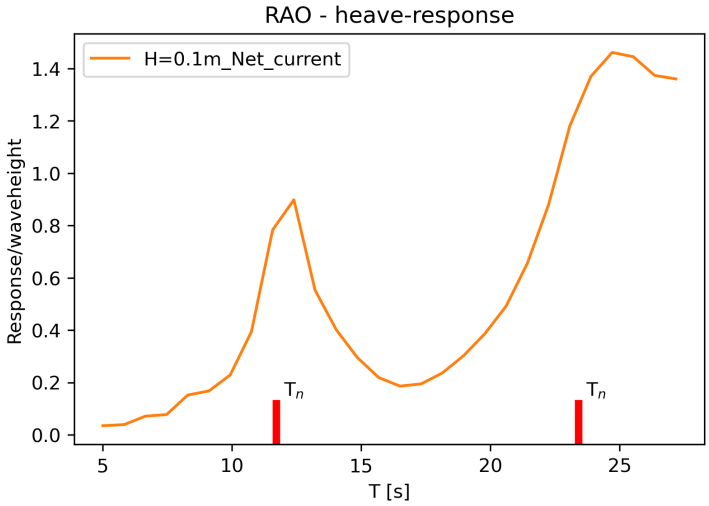

Figure 6.11: RAO, H = 0.1m, Current = 0.75 m/s Net pens

Figure 6.11 shows the RAO of the net pen model. It was acquired using the same method as before, using regular waves with 28 different periods and a waveheight of 0.1m, and a small current of 0.75 m/s. Again 700 seconds is simulated and the first 300 seconds are discarded. It is very similar to the model without net pens. The natural periods found from the decay test is shown as two red bars. It can be seen that the peaks are slightly to the right of these bars i.e. corresponding to larger periods. Looking back at Equation 6.1 in can be seen that an increase in weight corresponds to an increase in the natural period in heave. The net also gives a larger waterline area, but this is negligible.

A side by side comparison of the results from both models are given in Figure 6.12, with the results from the decay test again shown as red bars.

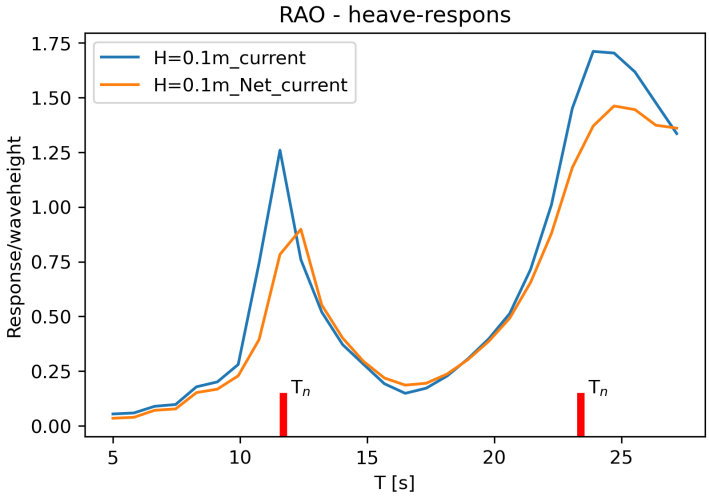

Figure 6.12: RAO, H = 0.1m, Comparison of the models, Current = 0.75m/s

There is good compliance between the two models. Again it can be seen that the natural periods are shifted towards the larger periods. There is also a reduction in amplification for the natural periods, probably stemming from the increased damping related to the drag forces on the net.

It should be noted that simulations using the net model are considerably more computationally taxing. The full set of simulations needed to create the RAO took more than 16 hours running on a desktop computer with an intel I7-4790k 4GHz processor. For comparison the no net model took just over one and a half hours to finish. It is therefore good that there is little difference between the two RAOs, since it means it's possible to analyse the structure using only the no net model. This however somewhat devalues the work done by Vegard Holen in modeling the net. However further investigations into behaviour of the net model should be done before concluding.

6.2.3 Changes in the wave height

Under the effect of small wave height and current the models behave very similarly. However a change in waveheight might change that. With a larger wave height, the importance of viscous forces should be of larger importance, according to figure 6.13. It's important to investigate this since the structure will be subjected to larger waves than 0.1m.

The same procedure is followed, this time subjecting both models to regular waves with a wave height of 1m. The wave period varies from 5s to 27.18s, with steps of 0.82s. The models are also subjected to a current with a velocity of 0.75m/s.

Figure 6.14 shows little difference between the two models. However for the larger periods the net model seems to have a smaller amplification. This is very similar to the results presented in Figure 6.12. The results are shown all together in Figure 6.15

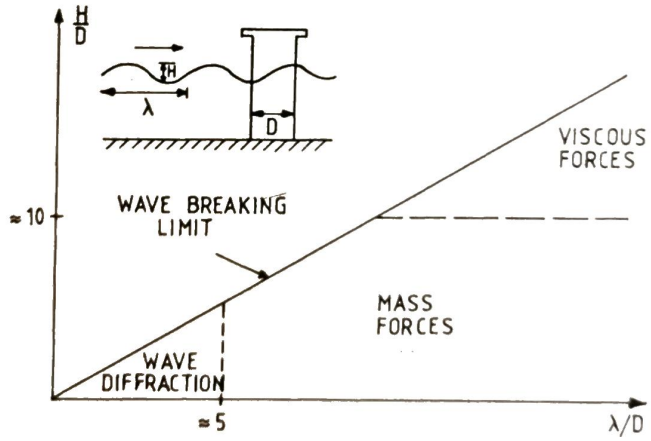

Figure 6.13: Rough classification of when different load components are of importance.

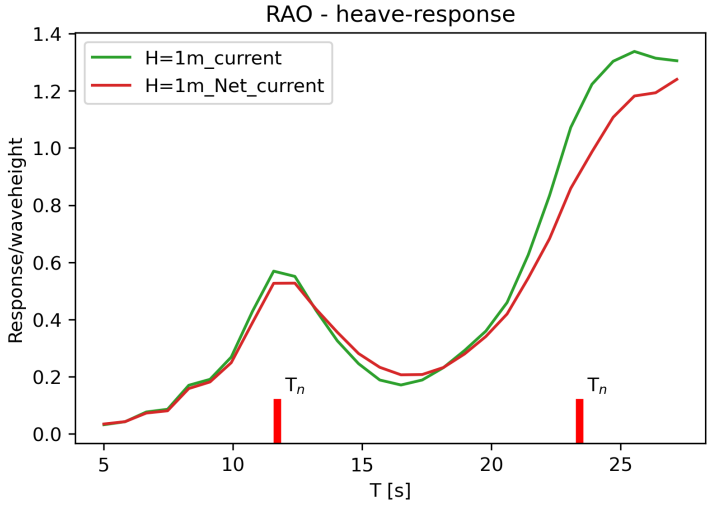

Figure 6.14: RAO, Waveheight of 1m, Current = 0.75 m/s, Comparison of net vs. no net

Aside from the area around the natural periods the amplification is close to consistent for all the models. However the amplification around the natural periods is reduced when the wave height is increased from 0.1 m to 1 m. The net models also has a reduced amplification compared to the no net models. The reduction in amplification could be explained by an increase in drag related damping. When the wave height increases so does the response, as well as the velocity of the structure. Damping is dependent on the velocity between the structure and water particles. Specifically the drag term in Morison's equation is proportional to the square of the velocity. A small increase in velocity could therefore lead to a large increase in drag related damping.

It should be noted that current also adds to the drag damping of the structure. The current used in these simulations is small and should not lead to a large damping force. This is true when the wave height is 1m. However, while the current is small, when the response is small the loss in energy due to damping can be significant. When the wave height is only 0.1 m the response is very small. An investigation into the significance of current damping should be undertaken.

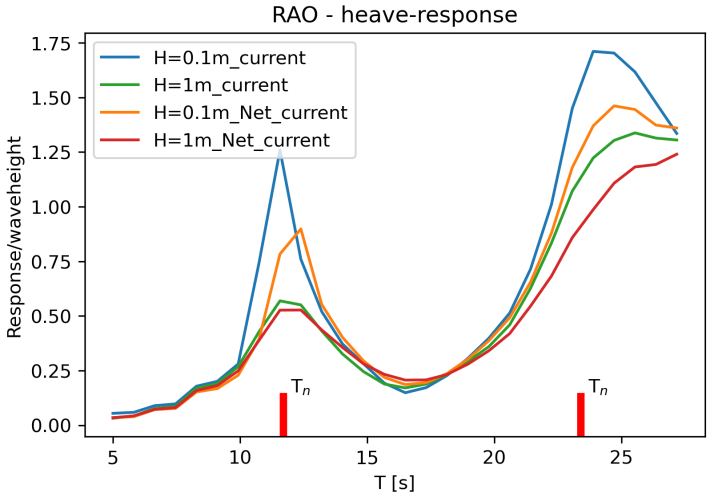

Figure 6.15: RAO, Current = 0.75 m/s, Comparison of wave heights

6.2.4 Measuring points

In the previous sections all the results were measured close to the longitudinal center of the structure at the point 4024. Since there is no easy way of establishing the flotation point of the structure, the flotation point being the point the structure rotates around, there will be some effect of pitch in the results. A different way of measuring the heave motion of the structure is taking the mean value of the front and aft heave motion. The measuring points are shown in Figure 6.16

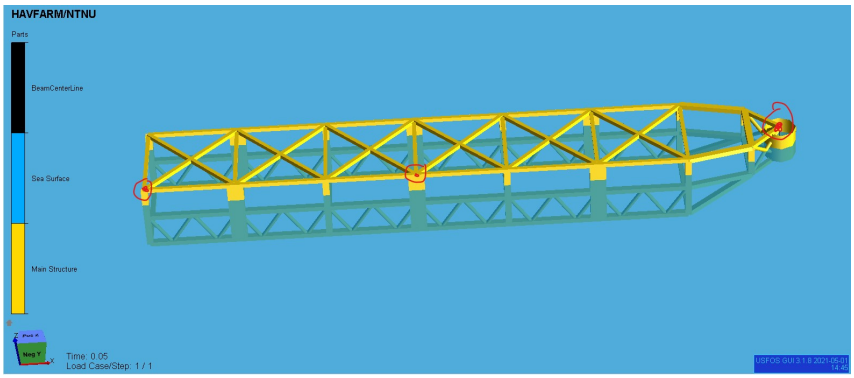

Figure 6.16: Position of the measuring points.

In order to discern if there is any noticeable difference in results between these methods, a set of simulations was ran both with and without net. The RAO of each model is shown in Figure 6.17 and 6.18.

As can be seen from these plots both models show that there are small differences for the smallest periods, but only slightly. From this one can infer that it is unnecessary to make changes at this stage by instead measure the mean heave motion.

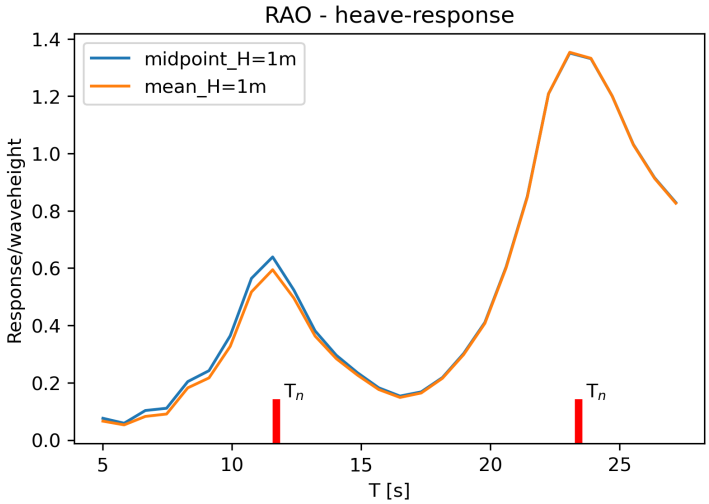

Figure 6.17: Difference between measuring points, without net pens, H = 1 m

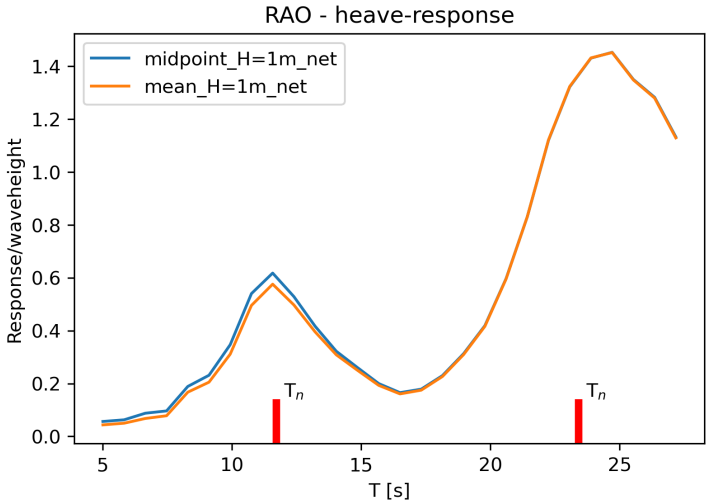

Figure 6.18: Difference between measuring points, with net pens, H = 1 m, without current

6.2.5 The significance of current

The effect of current was discussed at the end of subsection 6.2.3. It would be interesting to see the difference with and without current, on both large and small wave heights. The thought behind having current in the simulations originally was that at location the structure will be subjected to current as well as waves.

In order to investigate the effect of current on the response several simulations were run. Initially both the model with and without net was subjected to just regular waves with amplitude of only 0.1m. The periods again vary between 5s and 27.18 s. The results of the no net model is shown in Figure 6.19, together with the result of the same model with current.

Immediately it is observable how important the current damping is in this case. The amplification is much larger and more sporadic than previously. It even dips down close at one of the natural periods. Looking back at discussion surrounding the initial simulations, one can recognize the presence of transient motion in these results. The time history of the heave motion for this case is shown in Figure 6.20.

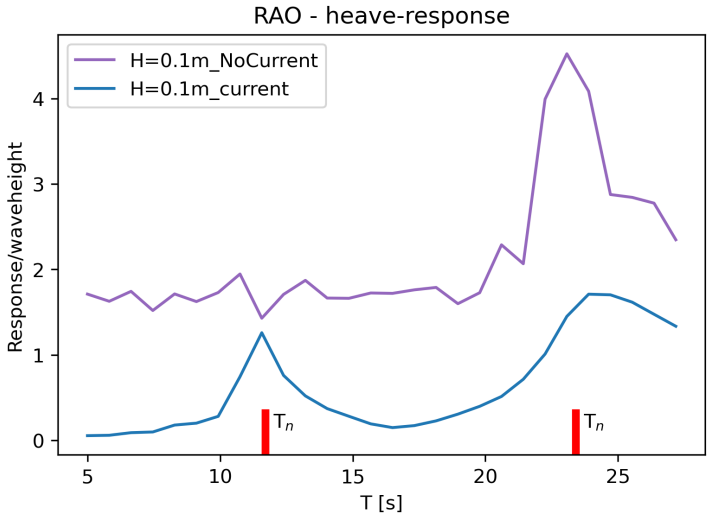

Figure 6.19: H=0.1m, No net, Current vs. No current

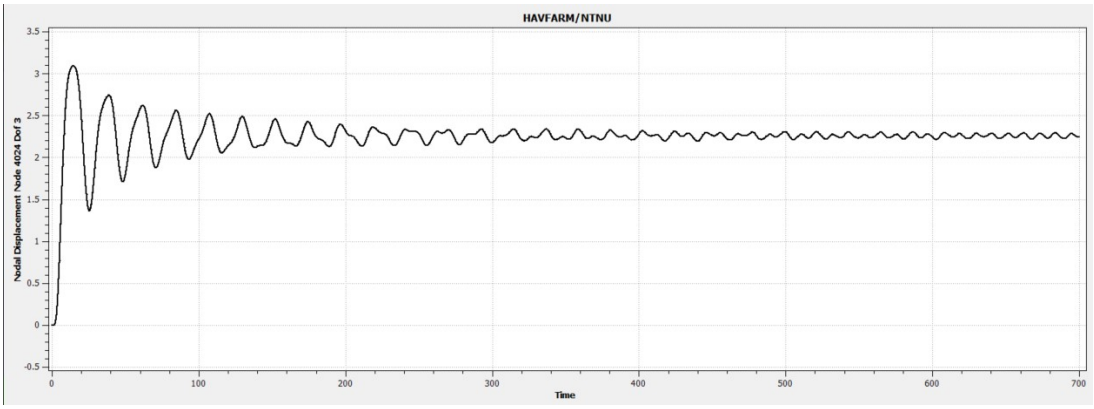

Figure 6.20: H=0.1m, T = 5.82 s, No net, Time history of the heave motion

From the time history we can see that not only is the heave motion very small, at 300 seconds into the simulation there is still much transient motion. In order to account for this the simulation should be run for longer, and a later cutoff point should be chosen for the data. What is also observable is that there is significantly more motion in this time history compared to Figure 6.9.

A set of longer simulations were run for 1000 seconds. Different cutoff points are shown in Figure 6.21 together with the results with current.
It seems the peaks are shifted towards smaller periods, compared to the results from the model with current. This is explainable by the fact that the encounter period has changed, since there is no longer a current. However this does not explain why the natural periods are smaller than the ones found in the decay test. There is not a significant difference however, and can be down to round off error.

The amplification is smaller and less sporadic when the cutoff is at 700s and 900s. These two RAOs are very consistent with each other. There is still more amplification than what is found for the model with current. This shows that for very small wave heights even small current adds a lot of damping to the structure.

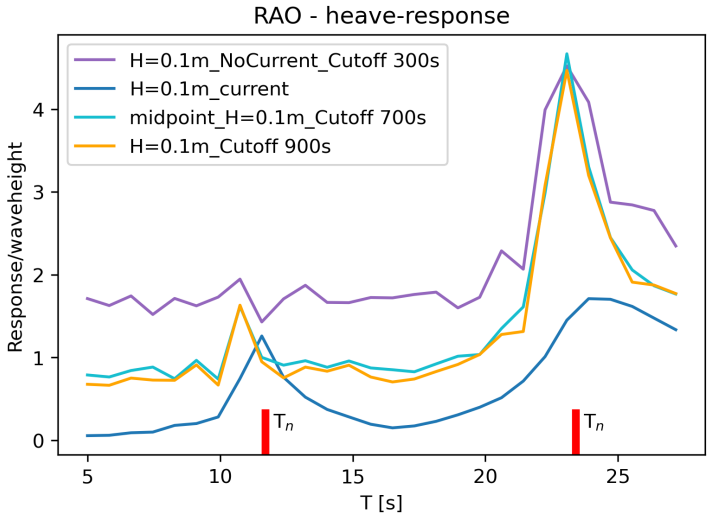

Figure 6.21: H=0.1m, No net, Comparison of cutoff and current

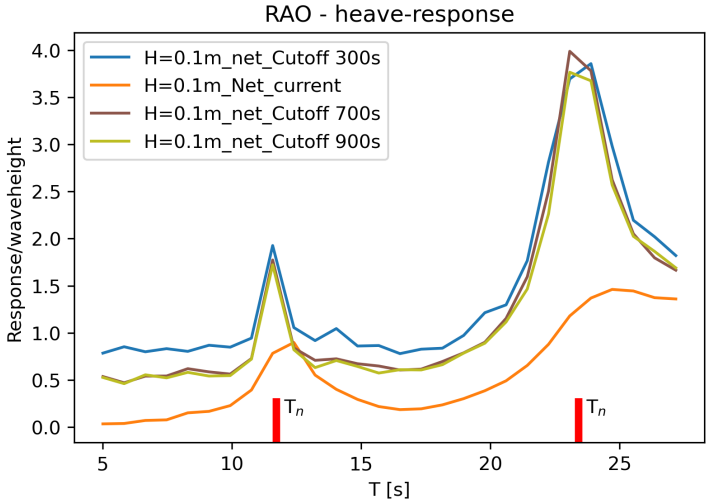

Figure 6.22: H=0.1m, Net, Comparison of cutoff and current

Net pen model

The same procedure was undertaken using the net model. The results are shown in Figure 6.22.

The effects of removing the current is very similar to that of the no net model. There is an increase in amplification across all periods. However there is no stark difference between the different cutoff times, at least not around the natural periods. This illustrates the dampening effect of the net pens, the transient motion dies out faster. Again the peaks are shifted towards smaller periods, which can be explained by the change in encounter period.

In Figure 6.23 the results from both models without current is shown. It shows that the RAOs overlap greatly when there is no current. However the amplification is much larger than before. So even though the relative difference in amplification is not that large, the actual difference is considerable. The difference in natural period is also noticeable. If we were to use the RAO of the no net model in order to estimate the q-probability response the result can be said to be representative. However the worst sea state is slightly different due to the shift in natural period. This shift though, is not substantial.

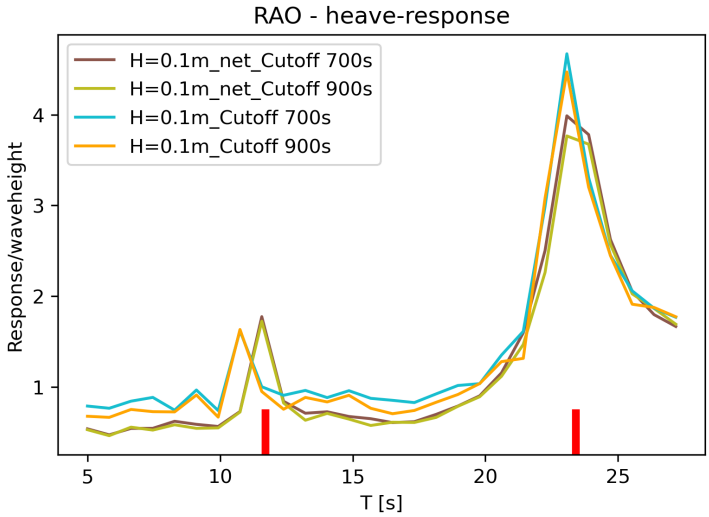

Figure 6.23: H=0.1m, No net, Comparison of cutoff for both net and no net

Change in wave heights

Having looked at the effect of current when the wave height is only 0.1m it is interesting to see if it has any effect when the wave height is larger i.e. 1m. Presumably the peaks should be shifted due to the change in encounter period. But since current velocity is small compared to the velocity of the heave motion, damping due to current should be relatively small.

Figure 6.24 shows the results of regular waves with 1m wave height, for both models, with and without current. As expected, the current seems to reduce the amplification around the natural periods as well as shift the peaks towards larger periods. There is only a slight reduction in amplification at the first peak, but the second shows larger reduction, although only for the net model. The shift in natural period is also more pronounced at the second peak. In this case it would have been useful to run more simulations of regular waves with larger periods, as the peak seems to have shifted outside the simulation range.

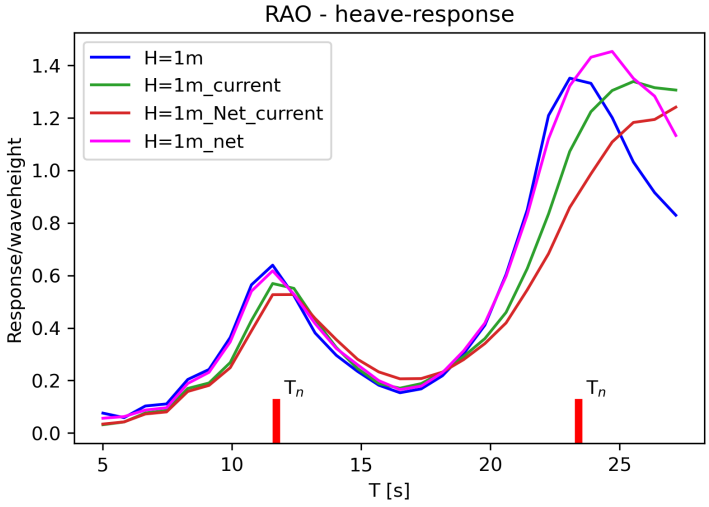

Figure 6.24: H=1m, Both models, Comparison of current vs. no current

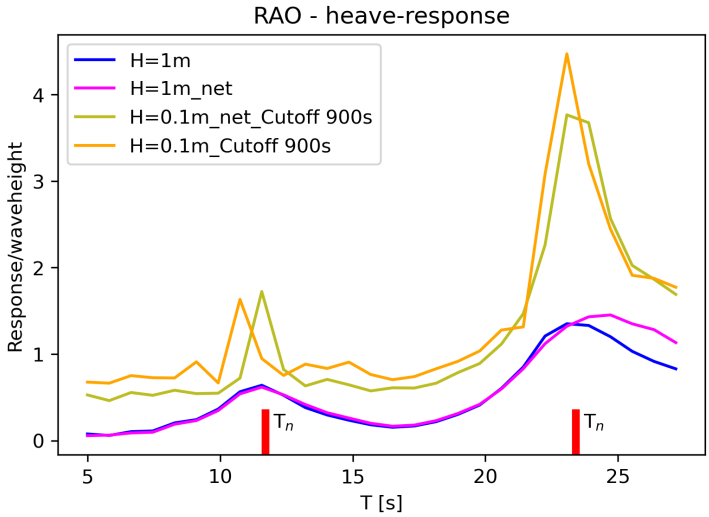

Figure 6.25: Both models, Comparison of wave heights without current

In Figure 6.25 the RAOs for both models, without current are shown together. The results of the no-net model is representative of the net model, or will at least give conservative results. In this conservative means larger, as estimating to small a response would be not conservative. The second peak is larger for the net model, but this falls outside of the range of the wave periods the structure is likely to encounter, which is 4-20 s [8].

Conclusions

The effect of current is most important when the wave height is small. When using a wave height of 0.1m both models showed a distinct reduction in amplification when also affected by a current of 0.75 m/s. When using regular waves with a height of 1 m, the reduction was still noticeable, but not as distinct, at least in the case of the no net model. In both cases the current speed was only 0.75 m/s. It could be interesting to also look at the effect of different current speeds in future.

The peaks in the RAO of both models are shifted towards smaller periods due to the change in encounter period. This shift is small and not significant.

6.2.6 Regular waves with 6 meter wave height

The only known information about the location is that the significant wave height used in design is 6 m. It has also been established that the RAO of the structure in heave has a peak at around 11.7 seconds. We can use this as an analogy to the worst sea state found using the contour line method. The worst sea state is then represented using a JONSWAP spectrum with a significant wave height, H_s, of 6 m, and a peak spectral period, T_p of 11.7. We then find the response spectrum using equation 4.8.

This method requires that there is a linear relationship between the response and wave height. As has been shown when investigating the model behaviour, the transfer function (RAO) changes with changes in the wave height. This is evidence of non-linear behaviour and therefore analysis in frequency domain is not valid. However, the RAO is valid for the wave height it is established for. Using it to estimate the response to waves with small differences in wave height should

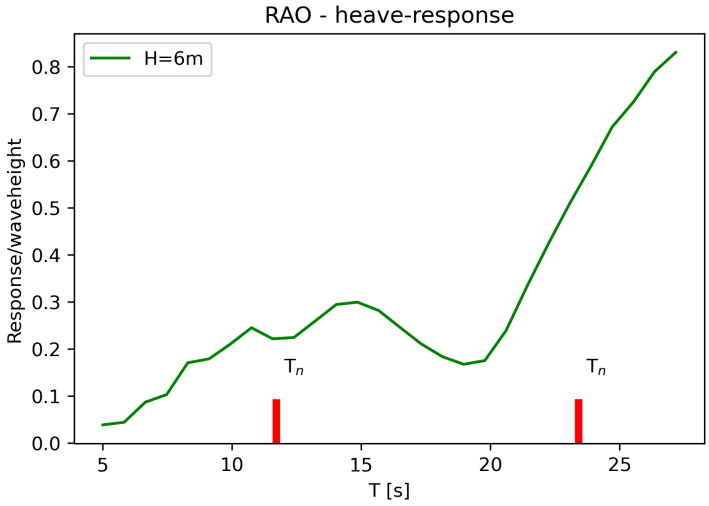

Figure 6.26: RAO, H=6m, No net model

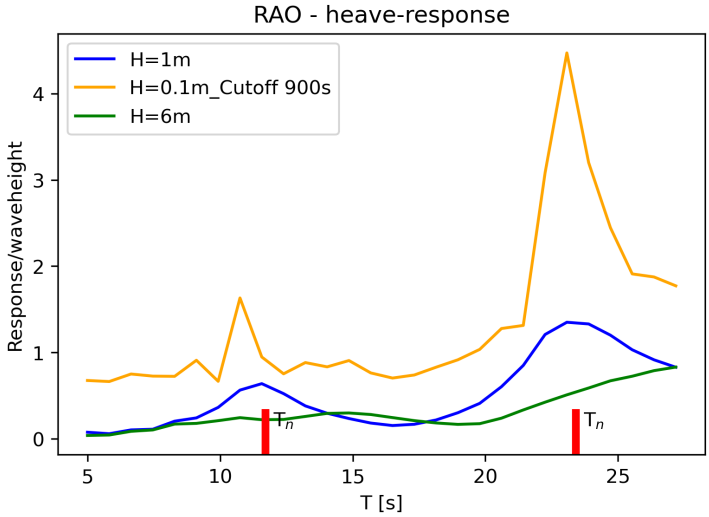

Figure 6.27: H=1m, Both models, Comparison of current vs. no current

give small errors. It can be said that an RAO is a type of linearization of the relationship between response and wave heights close to the one used to establish it. Therefore when using a significant waveheight of 6 m, the RAO should be established using regular waves with a wave height of 6 meters.

The RAO corresponding to regular waves with a wave height of 6 m is presented in Figure 6.26. Only the no-net model has been subjected to 6 m waves. It is assumed that the differences between the two models are negligible based on the previous results. Also as previously stated, simulation using the net-model is considerably more computationally taxing.

There has been a considerable reduction in amplification for all periods. The first peak observed previously is almost gone. The peaks are also even more shifted towards larger periods, so much that the second peak is outside of the simulation range.

In Figure 6.27, the results of the no net models for different wave heights are shown together. The most prominent change compared to the RAOs of the previous wave heights is the reduction

and almost removal of the first peak in the plot. H = 6m surpasses H = 1m at around 15 s, showing how the peak has been shifted. Besides this one can see that across all periods the amplification is reduced.

Why it is that the peaks are so considerably shifted cannot be explained using linear theory alone. The assumption is that the larger wave heights also induce larger motions, both in heave and pitch. This means a larger relative velocity between the water particles and the structure. The drag term in Morrison's equation, Equation 5.1, is proportional to the square of the relative velocity. This means a small change in relative velocity has a large effect on the damping. The damped eigenperiod, expressed in Equation 4.27, will increase with increased damping. This explains the shift of the peaks towards larger periods since resonance will be found at this period.

Based on these results its clear that to undertake a frequency domain analysis, one cannot use the RAO based on 1 m wave height. That would give a too large maximum response. Additionally the worst sea state is not the one outlined earlier, where $T_p = 11.7$s, but closer to 15 seconds.

6.3 Stochastic analysis in frequency plane

The method of stochastic analysis in frequency domain has been outlined in section 4.2.3. The proper transfer function has been established in subsection 6.2.6. The worst sea state is assumed to be the one where $H_s = 6$m and $T_p = 14.5$s. A standard JONSWAP spectrum is used to model the sea sate. This is shown in Figure 6.28 as a function of wave frequency.

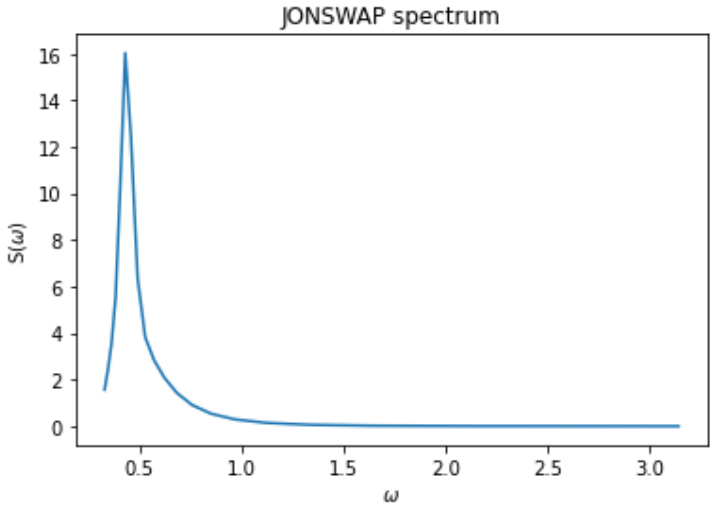

Figure 6.28: JONSWAP spectrum, $H_s = 6m$, $T_p = 14.5s$

For this sea state $\frac{T_p}{\sqrt{H_s}} = 5.9$. Recall from subsection 4.3.1 that the the upper limit for use of the JONSWAP spectrum is 5. Therefore use of the JONSWAP spectrum here is not an accurate representation of reality. Using it will result in a to high peek around T_p. This should lead to large waves with periods close to T_p. Since the transfer function has a peak close to T_p as well this should lead to larger excitation. Therefore it is arguable that use of the JONSWAP spectrum in this case is conservative, or at least not non-conservative.

The response spectrum is found according to Equation 4.8 using the RAO based on 6 meter wave height. This is shown in Figure 6.29.

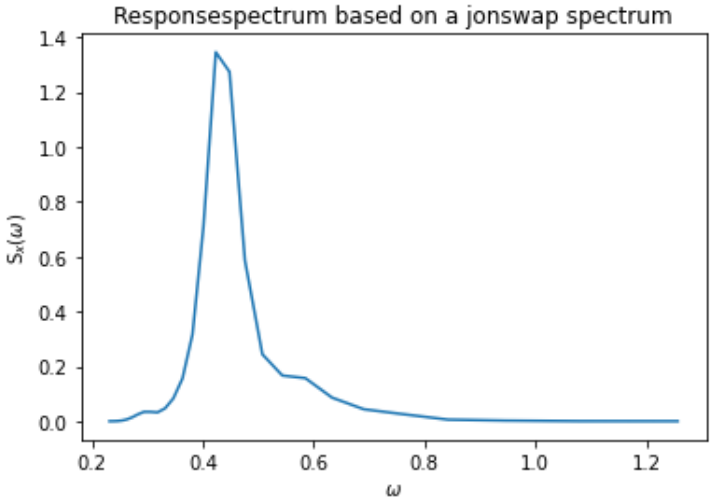

Figure 6.29: Response spectrum, $H_s = 6m$, $T_p = 14.5s$

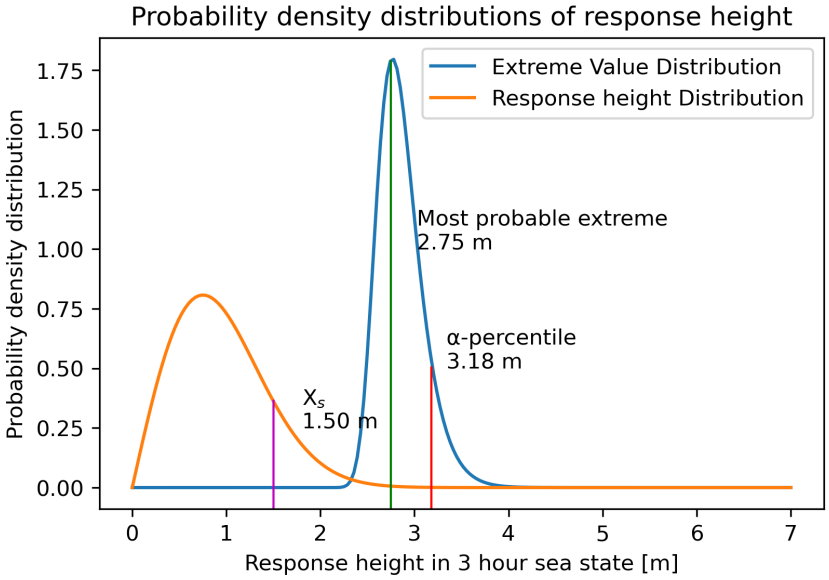

Figure 6.30: Response height distribution, $H_s = 6m$, $T_p = 14.5s$

This spectrum can be transformed into a probability density function for the response height. The response height will be Rayleigh distributed, and its distribution is shown as the orange graph in Figure 6.30.

The distribution of the maximum response height in the sea state is then found according to Equation 4.9. The distribution of the largest wave height in the sea state will be close to Gumbel distributed and is shown as the blue graph in Figure 6.30.

The goal is to determine the maximum response height in the worst sea state along the q-probability contour line. This value is often named the α-percentile, the value which has a probability of $1 - \alpha$ of being exceeded. For ULS assessment the value of α should be taken as $85 - 90\%$, and for ALS: $90 - 95\%$ [10]. The result found using a value of 90% was a maximum heave response height of 3.18 m.

6.4 Stochastic analysis in time domain

As was discussed in subsection 6.2.6, frequency domain analysis is predicted not to yield accurate results when the structure is subjected to non-linear effects. In this situation one should employ time domain analysis. To recap, the methodology consists of simulating multiple irregular sea states in order to establish a distribution of the largest response. Then find the α-percentile using the same method as in frequency domain analysis.

The irregular sea state is modeled in USFOS using a spectrum. In comes with two options as standard, PM or JONSWAP. As before the JONSWAP spectrum is assumed to best represent the location.

When calculating the component wave amplitudes, how the spectrum is discretized is important. A central question is how the upper and lower limit of the integration terms should be determined. USFOS offers two methods[22]:

1. Constant angular frequency width, $\Delta\omega$, i.e. $\omega_{u,j} - \omega_{l,j} = \Delta\omega = \frac{\omega_{u,j} - \omega_{l,j}}{N}$ where N is the number of regular waves, and $\omega_{u,j}$,$\omega_{l,j}$ the upper and lower bound respectively.

2. Adjusting the limits so that each wave component contains the same energy, known as equal are method. This has the effect that each wave component has the same amplitude, but that there are more frequencies corresponding to the energy rich part off the spectrum.

The argument for the equal area method is that the energy rich parts of the spectrum are the most important for the representation of the irregular sea. To properly represent the sea state one should put an emphasis on these frequencies[11].

Another important question is how many waves should the irregular wave consist of. After conferring with supervising professor Jørgen Amdahl, he recommended using the equal area method with 30 components.

It is important to point out that the spectrum contains all the information about a sea state, however a realization does not. It is only one of many possible realization. In order to establish the proper distribution of the largest response in the sea state sea state, it is necessary to run several time domain simulations. Haver[10] recommends a minimum of 20 simulations, in this case 30 has been used. More is preferable in order to get an accurate estimate. In order to differentiate between the realizations the starting seed is change between each run.

The worst sea state has been established previously by subjecting the model to regular waves with varying wave heights and wave periods. The worst sea state is taken to be a 3 hour period, where the significant wave height, H_s is 6m and the peak spectral period, T_p is 14.5s. Proper procedure dictates that multiple sea states are simulated in order to establish the worst sea states. This has been neglected here due to time and computational constraints.

USFOS handles most of the work when undertaking this type of analysis. The user has to define the type of analysis in the control file and change the seed between each simulation. A python script has been written in order to set up the necessary file system and file input to the analysis. The script also runs several USFOS simulations in parallel in order to minimize computation time. When the simulations are finished the time histories of the measured quantities are extracted using the USFOS module dynRes. The quantities has to be specified before hand in the control file. Running 30, 3 hour simulations of the no net model in irregular sea took approximately 27 hours.

When the simulations are finished, the largest amplitude in the time history of each realization is calculated. The collected sample of largest response heights are then fitted to a Gumbel distribution using the method of moments. The α-percentile is then found from this distribution.

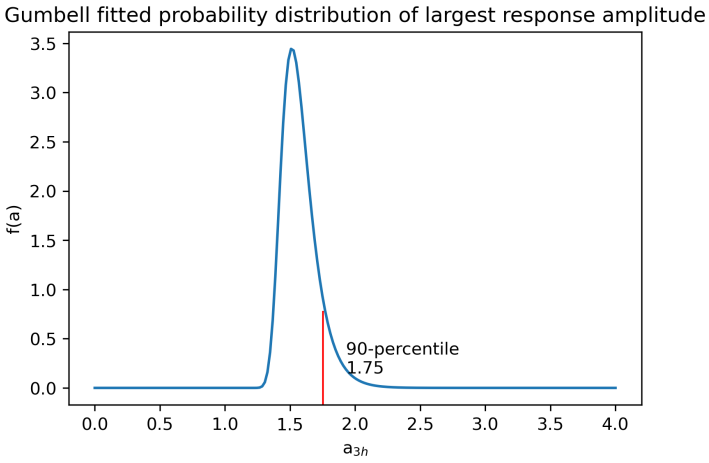

Figure 6.31: Distribution of the largest response amplitude, $H_s = 6m$, $T_p = 14.5s$, 3 hour duration

Figure 6.31 shows the Gumbel distribution fitted to the sample. This is the distribution of the amplitude not the response height. The α-percentile found from this distribution is an amplitude of 1.75m or a response height of 3.50m.

6.4.1 Comparison between frequency and time domain

In Figure 6.32, the extreme value distribution found using both methods are shown together. The distributions have a similar shape, thought the time domain distribution is shifted to larger heights and with a shorter peak.

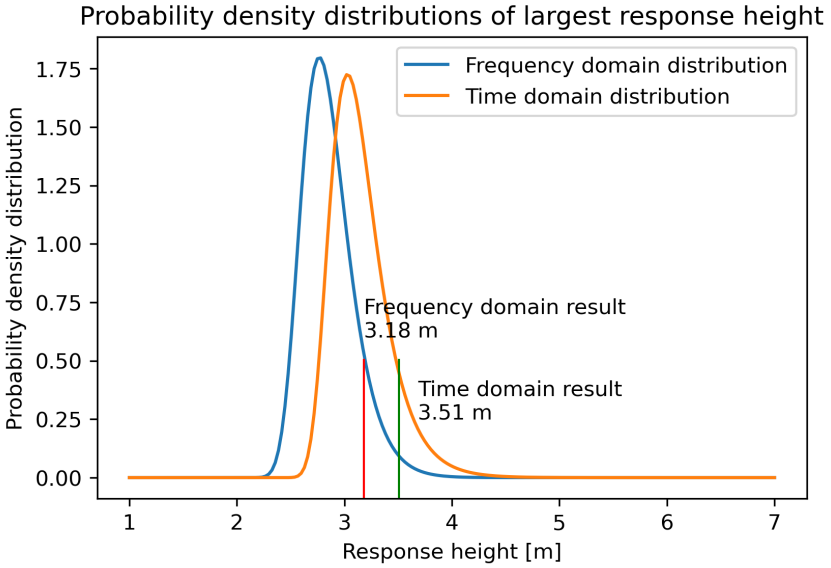

Figure 6.32: Comparison of extreme value distributions, $H_s = 6m$, $T_p = 14.5s$, 3 hour duration

Compared to the result from the frequency domain analysis the increase in α-percentile is about 10%. That is not a large change, but still significant. In this case the use of frequency domain analysis gives non-conservative results. This demonstrates that for structures dominated by non-linear loads, time domain analysis is necessary to obtain conservative results. This does not show that the results are accurate however. This depends upon whether the modeling decisions are correct.

While there is a significant difference, it is interesting that the results are so close. This could show that use of frequency domain analysis is still useful e.g. in the design stage, even though the structure is dominated by non-linear loads.

A characteristic heave response of 3.51m cannot be said to be of large significance. Assuming that the heave motion has a period equal to the spectral peak period (the average zero up-crossing period would have been better to use, but has not been calculated for the sample) the acceleration amplitude can be calculated as:

$$\ddot{\eta}_{3a} = \eta_{3a} \cdot (\frac{2\pi}{T_p})^2 \tag{6.4}$$

where η_{3a} is the heave amplitude. This gives an acceleration amplitude of $0.33 m/s^2$ which is tiny. This of course, assumes the structure has a harmonic motion which is not correct, but it still gives an indication of the size of the acceleration.

In the end it seems that heave motion of the structure is not a critical response with respect to the safety of the structure. It is stated DNVGL-RP-C103[5] when discussing the vertical acceleration of the deck mass, that: “This response is in most cases not critical for any global structural element in submerged conditions... Typical maximum values in survival condition are 0.2-0.25 g.” The result of the analysis is in agreement with the standard.

Only one sea state has been investigated based on results found from regular wave analysis. While this should give a good indication about the worst sea state, it would be wise to run simulations for other sea states as well. In addition use of the contour line method is preferable. As was previously stated, only the significant wave height was known when undertaken this analysis. However, late in the project a scatter matrix showing the distribution of the long term parameters were obtained. Due to time limitations, this information was not utilized.

Chapter 7

End remarks

Presented in this section is a summary of the findings of this thesis. In addition, suggestions and recommendations for future work related to analysis of Havfarm 1 are given.

7.1 Conclusions

A brief review of previous work done on offshore fish farms have been presented. Among these the work of Vegard Holen[11] has been the most useful. A short review of current rules and regulations governing offshore fish farms has also been carried out. It was found that the rules presented by the classification society DNV GL are the most applicable and up to date.

An overview of the limit state design philosophy and related methods is presented. The focus has been placed on several methods of establishing ULS utilization and their applicability to analysis of Havfarm 1. It was found that Havfarm 1 should be analysed using stochastic analysis methods, such as the metocean contour line method.

Dynamic analysis of the Havfarm 1 concept has been undertaken using methodology related to ULS design. The analysis is based on a model of Havfarm 1 created by Vegard Holen. The model was found to be lacking in certain aspects and not representative of the final structure.

Focus was put on the heave motion of the structure. It was previously found that the model is overdimensioned with respect to yield utilization, ($<< 1$). Focus was therefore put on other characteristic responses. In the end it was found that the model is not at risk of experiencing critical heave motion.

With respect to the heave motion it was found that the structure can be modelled without the net in dynamic analysis and still get representative results. This meant the computation time could be decreased considerably.

In terms of damping the model is largely drag dependent. Therefore the dynamic response of the structure is highly non-linear. In order to get accurate results from a dynamic analysis the model should be analysed using time domain methodology. Both frequency domain and time domain analysis was undertaken. A 10% increase in the extreme heave motion was found when comparing the frequency domain to the time domain result. This significant increase explains why one should employ time domain analysis.

7.2 Recommendations for further work

These are suggestions and recommendations for anyone interested in further investigating this structure. It is assumed that the reader will have access to the model files and long term description of the sea state parameters of the location.

If one decides to investigate this structure further it would be prudent to make changes to the model. To make comments on the finished structure one should change the model to reflect the final design. Primarily the bow section should be changed, but also the cross sections. In this thesis no focus was put on stress or strains in the structural elements, primarily due to the way the bow section and the cross sections are modeled. Other modeling changes could be to employ a catenary model instead of a spring model for the mooring lines.

Both the results of this thesis and Vegard Holen's thesis suggest that ULS analysis of the structure is not critical. The structure seems to be able to handle any extreme loads it is expected to experience at the location. It would be more interesting either to look at accidental loads; such as ship impacts, or failure due to fatigue.

If one where to undertake ULS analysis, use of the contour line method is recommended, with information from the location. Possible failure modes could be mooring line snapping, rupture of the net, or roll motion due to deviation between fish farm heading and direction of incoming waves.

A way to validate the results would be welcome. It was initially envisioned that the results of this project could be compared with data acquired by 7waves. However this did not come to fruition. If at all possible, cooperation with 7waves or others would be recommended in future.

Through use of USFOS it was found that the program functions well. It is well behaved in that no bugs were encountered , and the only errors encountered were due to user error. No modelling has been done using USFOS in this thesis, besides making removing the net form preexisting model. Therefore no comment can be made on that subject. However, if the user is familiar with programming in python or similar there should be no problem. Therefore, use of USFOS on future projects connected to Havfarm1, can be recommended. On the other hand, use of a different structural analysis program might be better the option. If so, verification of the results obtained in USFOS by comparison with results from another program should be undertaken. It should be up to the individual to choose what program they wish to use.

It would also be recommended for future master students to read up on, and make frequent use of the recommended practises and standards related to offshore fish farms. These contain a lot of useful information, and will be most likely encountered at later stages in their careers.

Bibliography

[1] Pål T. Bore, Jørgen Amdahl, and David Kristiansen. "Modelling of hydrodynamic loads on aquaculture net cages by a modified morison model". In: *7th International Conference on Computational Methods in Marine Engineering, MARINE 2017* 2017-May (2017), pp. 647–662.

[2] Pal Takle Bore and Jørgen Amdahl. "Determination of environmental conditions relevant for the ultimate limit state at an exposed aquaculture location". In: *Proceedings of the International Conference on Offshore Mechanics and Arctic Engineering - OMAE* 3B-2017 (2017), pp. 1–14.

[3] Pal Takle Bore, Jørgen Amdahl, and Martin Slagstad. "ACCURACY OF SIMPLIFIED METHODS FOR FATIGUE DAMAGE ESTIMATION OF EXPOSED FISH FARMS". In: *Proceedings of the International Conference on Offshore Mechanics and Arctic Engineering - OMAE* (2020), pp. 1–10.

[4] DNV-GL. *DNVGL-OS-C101 Design of offshore steel structures, general - LRFD method*. 2019.

[5] DNV-GL. *DNVGL-RP-C103 Column-Stabilised Units*. 2015.

[6] DNV-GL. *DNVGL-RU-OU-0503 Offshore fish farming units and installations*. 2020.

[7] DNV-GL. *Environmental conditions and environmental loads*. 2010.

[8] O M. FALTINSEN. *Sea Loads on Ships and Offshore Structures*. Cambridge: Cambridge University Press, 1990. ISBN: 0521458706.

[9] *Forskrift om krav til teknisk standard for flytende akvakulturanlegg (NYTEK-forskriften) - Lovdata*. 2011. URL: https://lovdata.no/dokument/SF/forskrift/2011-08-16-849.

[10] Sverre Haver. *METOCEAN MODELLING AND PREDICTION OF EXTREMES*. Draft vers. March. Stavanger, 2019.

[11] Vegard Holen. *Ultimate Limit State Analysis of Havfarm*. 2017.

[12] Ivar Langen and Ragnar Sigbjörnsson. *Dynamic Analysis of Constructions(English translation)*. 1979.

[13] Carl M Larsen et al. *Marine dynamics: TMR 4182 marine dynamics, Department of Marine Technology, Faculty of Engineering Science and Technology, NTNU*. Trondheim, 2019.

[14] M M Lee and A T Chwang. "Cite as". In: *Physics of Fluids* 12 (2000). DOI: 10.1063/1.870284. URL: https://doi.org/10.1063/1.870284.

[15] Torgeir Moan. *Design of Marine structures Vol. 1*. Trondheim, 1994.

[16] NORDLAKS. *Havfarmen Jostein Albert — Nordlaks*. URL: https://www.nordlaks.no/havfarm/havfarm1.

[17] NORDLAKS. *Havfarmene og Nordlaks-metoden*. 2020.

[18] *Population projection by the UN, World, 1950 to 2100*. URL: https://ourworldindata.org/grapher/un-population-projection-medium-variant?tab=chart&country=~OWID_WRL.

[19] Standards Norway. *NORSOK STANDARD N-003 Actions and action effects*. OSLO, 2017.

[20] Standards Norway. *Norwegian Standard NS 9415.E:2009 Marine fish farms - Requirements for site survey, risk analyses, design, dimensioning, production, installation and operation*. 2009.

[21] USFOS AS. *USFOS product info*. URL: https://usfos.no/product_info/usfos/index.html.

[22] *USFOS Hydrodynamics Theory*. SINTEF, 2010. URL: http://www.usfos.no/manuals/usfos/theory/documents/Usfos_Hydrodynamics.pdf.

[23] *What is Overfishing? Facts, Effects and Overfishing Solutions*. URL: https://www.worldwildlife.org/threats/overfishing.

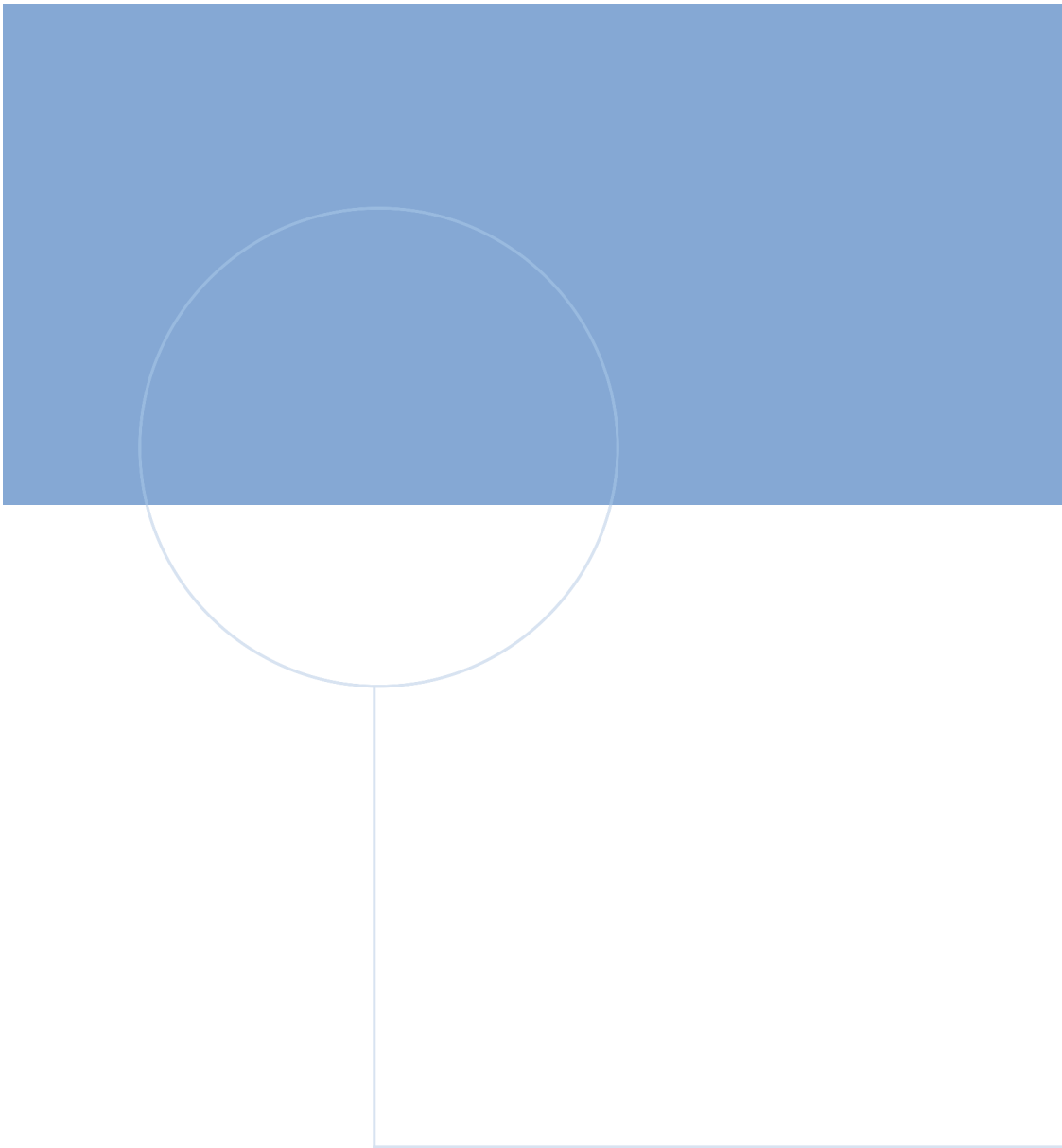

NTNU

Norwegian University of
Science and Technology